

Discovering Process Models With Long-Term Dependencies While Providing Guarantees and Handling Infrequent Behavior

Lisa L. Mannel ^C

Process and Data Science (PADS)

RWTH Aachen University

Aachen, Germany

mannel@pads.rwth-aachen.de

Wil M. P. van der Aalst

Process and Data Science (PADS)

RWTH Aachen University

Aachen, Germany

wvdaalst@pads.rwth-aachen.de

Abstract. In process discovery, the goal is to find, for a given event log, the model describing the underlying process. While process models can be represented in a variety of ways, Petri nets form a theoretically well-explored description language and are therefore often used in process mining. In this paper, we present an extension of the eST-Miner process discovery algorithm. This approach computes a set of Petri net places which are considered to be fitting with respect to a user-definable fraction of the behavior described by the given event log, by evaluating all possible candidate places using token-based replay. The set of replayable traces is determined for each place in isolation, i.e., they do not need to be consistent, which allows the algorithm to abstract from infrequent behavioral patterns. When combining these places into a Petri net by connecting them to the corresponding uniquely labeled transitions, the resulting net can replay exactly those traces that can be replayed by each of the inserted places. Thus, inserting places one-by-one without considering their combined effect may result in deadlocks and low fitness of

Address for correspondence: mannel@pads.rwth-aachen.de

^CCorresponding author

the Petri net. In this paper, we explore adaptations of the eST-Miner, that aim to select a subset of places such that the resulting Petri net guarantees a definable minimal fitness while maintaining high precision with respect to the input event log. To this end, a new fitness metric is introduced and thoroughly investigated. Furthermore, various place selection strategies are proposed and their impact on the returned Petri net is evaluated by experiments using both real and artificial event logs.

Keywords: Process Discovery, Petri Nets, eST-Miner, long-distance dependencies, non-free choice

1. Introduction and Related Work

More and more corporations and organizations support their processes using information systems, which record the occurring behavior and represent this data in the form of *event logs*. Each event in such a log has a name identifying the executed activity (activity name), an identification mapping the event to some execution instance (case id), a timestamp showing when the event was observed, and often extended meta-data of the activity or process instance. In the field of *process discovery*, we utilize the event log to identify relations between the activities (e.g., pre-conditions, choices, concurrency), which are then expressed within a process model, for example a Petri net [1, 2, 3, 4]. This is non-trivial for various reasons. We cannot assume that the given event log is complete, as some possible behavior might be yet unobserved. Also, real-life event logs often contain noise in the form of incorrectly recorded data or deviant behavior, which is not desired to be reflected in the process model. However, correctly classifying behavior as noise can be hard to impossible. An ideal process model can reproduce all behavior contained in an event log, while not allowing for unobserved behavior. It should represent all dependencies between events and at the same time be simple enough to be understandable by a human interpreter. Computation should be fast and robust to noise. Usually, it is impossible to fulfill all these requirements at the same time. Thus, different algorithms focus on different quality criteria, while neglecting others. As a result, the models returned for a given event log can differ significantly.

Many existing discovery algorithms abstract from the full information given in a log and/or generate places heuristically, in order to decrease computation time and complexity of the returned process models. While this is convenient in many applied settings, the resulting models are often underfitting, in particular when processes are complex. Examples are the Alpha Miner variants ([5]), the Inductive Mining family ([6]), genetic algorithms or Heuristic Miner [7]. In contrast to these approaches, which are not able to (reliably) discover complex model structures, algorithms based on region theory [8, 9, 10, 11, 12, 13, 14, 15, 16, 17, 18]) discover models whose behavior is the minimal behavior representing the input event log. On the downside, these approaches are known to be rather time-consuming, cannot handle noise, and tend to produce complex, overfitting models which can be hard to interpret. A combination of strategies has been introduced in [19], which aims to circumvent performance issues by limiting the application of region theory to small fragments of a pre-discovered Petri net.

In [20] we introduced the discovery algorithm eST-Miner. This approach aims to combine the capability of *finding complex control-flow structures like longterm-dependencies* with an inherent ability to *handle low-frequent behavior* while exploiting the token-game to *increase efficiency*. The basic idea is to evaluate all possible places, defined by all possible combinations of uniquely labeled transitions, to discover a set of fitting ones. A place can be considered fitting even if it disagrees with a part of behavior in the event log, which allows handling infrequent behavior. Efficiency is significantly increased by skipping uninteresting parts of the search space. This may decrease computation time immensely compared to the brute-force approach evaluating every single candidate place, while still providing guarantees with regard to fitness and precision.

While traditional region-theory uses a global perspective to find a set of feasible places, the eST-Miner evaluates each place separately, that is from a local perspective. This allows us to easily enforce all kinds of constraints definable on the place level, e.g., constraints on the number or type of connected transitions, token throughput or similar. In particular, we are able to filter infrequent behavior locally, by requiring each place to be able to replay only part of the traces in the event log. A candidate place will be accepted and inserted into the returned Petri net, if the event log contains sufficient support for the relation between the activities as defined by the place. In contrast to common noise filtering techniques which lose information by removing infrequent trace variants or infrequent activities from the event log, this approach can consider all information in the event log to discover relations between activities. In particular, we aim to accurately represent all activities with well-defined positioning within the process control flow, while ignoring chaotic behavior.

$$L = [\langle \blacktriangleright, x_1, x_2, x_3, y_3, y_2, y_1, \blacksquare \rangle^1, \langle \blacktriangleright, x_3, x_2, x_1, y_1, y_2, y_3, \blacksquare \rangle^1, \\ \langle \blacktriangleright, x_1, x_2, x_3, y_3, y_1, y_2, \blacksquare \rangle^1, \langle \blacktriangleright, x_3, x_1, x_2, y_1, y_2, y_3, \blacksquare \rangle^1, \\ \langle \blacktriangleright, x_1, x_2, x_3, y_2, y_3, y_1, \blacksquare \rangle^1, \langle \blacktriangleright, x_2, x_3, x_1, y_1, y_2, y_3, \blacksquare \rangle^1, \\ \langle \blacktriangleright, x_1, x_2, x_3, y_2, y_1, y_3, \blacksquare \rangle^1, \langle \blacktriangleright, x_2, x_1, x_3, y_1, y_2, y_3, \blacksquare \rangle^1, \\ \langle \blacktriangleright, x_1, x_2, x_3, y_1, y_3, y_2, \blacksquare \rangle^1, \langle \blacktriangleright, x_1, x_3, x_1, y_1, y_2, y_3, \blacksquare \rangle^1]$$

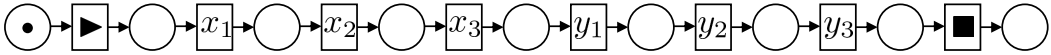


Figure 1. The example event log L exhibits mostly well-defined behavior corresponding to the sequential Petri net below. However, in all traces some deviations in activity order occur (marked in red). By simply removing infrequent traces or activities in a pre-processing step we cannot discover the underlying main process structure. This becomes even more challenging for processes that include concurrency, choice or non-free choice constructs.

Consider the simple example event log and Petri net in Figure 1. The event log exhibits mostly well-defined behavior corresponding to the behavior of the Petri net. However, in all traces some deviations in activity order occur (marked in red). Often, users do not want a discovery algorithm to return a model including all possible behavior in an event log but rather only the main process structure with noise or deviations filtered out. In this example, it is not possible to discover the main process behavior by simply removing infrequent traces or activities in a pre-processing step. In more

complex processes, exhibiting concurrency, choice or non-free choice constructs, this becomes even more challenging. However, the local perspective of the eST-Miner allows it to ignore deviating parts of a trace not involved with the place currently evaluated. Each place included in the presented Petri net is able to replay a large part of the presented event log and can therefore be discovered when considered in isolation.

The local perspective of the eST-Miner ensures that all occurrences of activities within a log are considered when discovering a model. However, when a set of discovered fitting places is combined into a Petri net, this Petri net allows only for the behavior in the intersection of the behaviors allowed by all inserted places. Thus, the Petri net may include deadlocks or dead parts, resulting in a much lower overall fitness than the fitness of each individual place and an overly complicated model. In extreme cases, the constructed net cannot replay any trace at all, as illustrated by the small example in Figure 2. Here, if we allow the insertion of places that replay only a small fraction of the traces in the event log, e.g., a fraction of 0.35, the Petri net discovered for the given event log cannot fire any transition after the start transition.

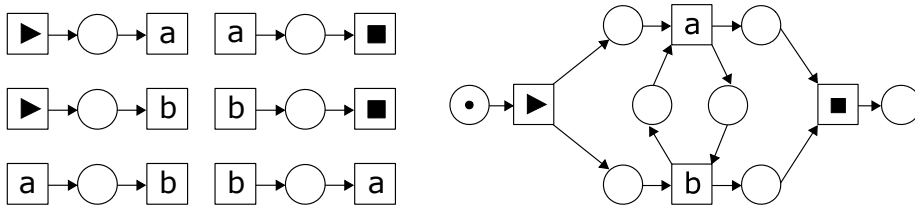


Figure 2. Consider the event log $L = [\langle \blacktriangleright, a, b, \blacksquare \rangle^{40}, \langle \blacktriangleright, b, a, \blacksquare \rangle^{60}]$ and the set of candidate places on the left. Assuming that we set the eST-Miner to accept all places that can replay at least 35 % of the event log, it would add all those places and return the Petri net on the right. Although each individual place has at least 40 fitting traces, the whole model cannot replay any trace.

In this paper, we aim to remedy this issue by investigating strategies of selecting a subset of places which can be combined into a deadlock-free Petri net with definable minimal fitness, while simultaneously striving for high precision and simplicity, without losing the desirable properties of the eST-Miner. Additionally, we introduce a new fitness metric used to evaluate candidate places with the goal to better control how candidate place selection affects infrequent behavior. We require the algorithm to maintain its ability to discover and model non-local dependencies and to provide guarantees without over- or underfitting. Furthermore, the time and space consumption should remain reasonable, in particular more scalable than classic region theory approaches.

This paper is a significantly extended and revised version of our work presented in [21]. With respect to our previous work, the main extensions are:

- Section 3 elaborated on the different candidate place sets and Section 4 details the problems related to interactions between places.
- In Section 5 we introduce a new fitness metric to handle infrequent behavior and thoroughly investigate its properties. In particular, we aim to maintain our algorithm’s ability to abstract from deviations and avoid overfitting, while at the same time preventing infrequent activities to

cause deadlocks in the returned Petri net. We explore the monotonicity properties of the new metric and show that it can be smoothly incorporated into the eST-Mining framework. This refines the place candidate evaluation and enables significant improvements of the eST-Miners approach to noise handling.

- We significantly extend the experimental evaluation of our previous work and provide an in-depth discussion of the results, in particular with respect to their interpretation in the context of the applied quality metrics. Furthermore, an analysis of the algorithm's running time is added.
- We extend and refine the preliminary definitions and concepts to make the paper self-contained. Furthermore, Section 4 provides a discussion of the context and assumptions we make, together with detailed examples and motivation for the proposed extensions and refinements. Examples and motivation are extended in other sections as well.

Section 2 provides basic notation and definitions. In Section 3, we briefly review the basics of the standard eST-Miner before providing a detailed problem description and method overview in Section 4. The newly introduced fitness metric and its incorporation into the eST-Miner framework are investigated in Section 5. Sections 6 and 7 present our place selection approach, followed by an extensive evaluation in Section 8. Finally, we discuss design choices, open questions and future work in Section 9 before concluding this work with Section 10.

2. Basic Notations, Event Logs, and Process Models

A set, e.g. $\{a, b, c\}$, does not contain any element more than once, while a multiset, e.g. $[a, a, b, a] = [a^3, b]$, may contain multiples of the same element. The intersection of two sets contains only elements that occur in both sets, i.e., $\{x, y\} \cap \{y, z\} = \{y\}$, while the intersection of two multisets contains each element with its minimum frequency, i.e. $[x, y^2, z] \boxplus [y^5, z^2] = [y^2, z]$. Similarly, the union of two sets contains all elements in both sets once, i.e., $\{x, y\} \cup \{y, z\} = \{x, y, z\}$, while the union of two multisets contains all elements with the sum of their frequencies, i.e. $[x, y^2, z] \boxplus [y^5, z^2] = [x, y^7, z^3]$. By $\mathbb{P}(X)$ we refer to the power set of the set X , and $\mathbb{M}(X)$ is the set of all multisets over this set. In contrast to sets and multisets, where the order of elements is irrelevant, in sequences the elements are given in a certain order, e.g., $\langle a, b, a, b \rangle \neq \langle a, a, b, b \rangle$. We refer to the i -th element of a sequence σ by $\sigma(i)$. The size of a set, multiset or sequence X , that is $|X|$, is defined to be the number of elements in X .

We define activities, traces, and logs as usual, except that we require each trace to begin with a designated start activity (\blacktriangleright) and end with a designated end activity (\blacksquare). Note that this is a reasonable assumption in the context of processes, and that any log can easily be transformed accordingly.

Definition 2.1. (Activity, Trace, Event Log)

Let \mathcal{A} be the universe of all possible *activities* (e.g., actions or operations), let $\blacktriangleright \in \mathcal{A}$ be a designated start activity and let $\blacksquare \in \mathcal{A}$ be a designated end activity. A *trace* is a sequence $\sigma = \langle a_1, a_2, \dots, a_n \rangle$ such that $a_1 = \blacktriangleright, a_n = \blacksquare$ and $a_i \in \mathcal{A} \setminus \{\blacktriangleright, \blacksquare\}$ for $i \in \{2, 3, \dots, n-1\}$. Let \mathcal{T} be the universe of all such traces. An *event log* $L \in \mathbb{M}(\mathcal{T})$ is a multiset of traces.

In this paper, we use an alternative definition for Petri nets. We only allow for places connecting transitions, called here activities, that are initially empty (without tokens), because we allow only for traces starting with \blacktriangleright and ending with \blacksquare . These places are uniquely identified by the non-empty sets of input activities I and output activities O . Each activity corresponds to exactly one uniquely labeled transition, therefore, this paper refers to transitions as activities.

Definition 2.2. (Places and Petri nets)

A *Petri net* is a pair $N = (A, P)$, where $A \subseteq \mathcal{A}$ is the set of activities including start and end, i.e., $\{\blacktriangleright, \blacksquare\} \subseteq A$, and $P \subseteq \{(I|O) \mid I \subseteq A \wedge I \neq \emptyset \wedge O \subseteq A \wedge O \neq \emptyset\}$ is the set of *places*. We call I the set of *ingoing* activities of a place and O the set of *outgoing* activities.

Note that if $p = (I|O)$, then $\bullet p = I$ and $p \bullet = O$ using standard notation.

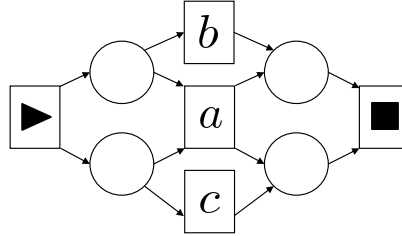


Figure 3. Example Petri net with $A = \{\blacktriangleright, a, b, c, \blacksquare\}$ and places $P = \{(\blacktriangleright|a, b), (\blacktriangleright|a, c), (a, b|\blacksquare), (a, c|\blacksquare)\}$.

Figure 3 shows an example Petri net with places represented by circles and activities represented by squares. A Petri net can *replay* a trace, i.e., a sequence of activities, by firing the corresponding transitions. A transition a can *fire* if and only if all places connected to it by an incoming arc ($\{(I|O) \subseteq P \mid a \in O\}$) have at least one token. We call such a transition *enabled*. Tokens are visualized by small black circles in places. The distribution of tokens in the places determines the state of the Petri net and is called a *marking*. When a transition fires, it consumes one token from every incoming place and produces a token in every outgoing place. In the example Petri net only the transition \blacktriangleright can fire initially, consuming a token from each place in its incoming set of places (which in this case is the empty set) and producing a token in $(\blacktriangleright|a, b)$ and $(\blacktriangleright|a, c)$. This enables transitions a, b and c .

A place is *fitting* with respect to a trace σ if it can replay σ without missing or remaining tokens. Otherwise, if it is missing tokens during replay we call it *underfed*, while a place with remaining tokens after complete replay of σ is called *overfed* with respect to the trace σ . Note that a place can be underfed and overfed with respect to a trace at the same time. Consider the example Petri net in Figure 3 and the trace $\langle b, \blacktriangleright, a, \blacksquare \rangle$. The place $(\blacktriangleright|a, b)$ is *underfed* with respect to this trace, because its outgoing transition b is fired while it has no token. The place $(\blacktriangleright|a, c)$ is *fitting* with respect to the trace, because it is not impacted by firing b , then firing \blacktriangleright produces a token, which is subsequently consumed when a is fired. Finally, The place $(a, b|\blacksquare)$ is *overfed*: the activity b produces a token here, \blacktriangleright has no impact, then firing activity a produces a second token. Firing \blacksquare at the end of the trace consumes only one of the two tokens, thus one token is remaining.

Definition 2.3. (Fitting, Underfed and Overfed Places, cf. [22])

Let $p = (I|O) \in \mathbb{P}(\mathcal{A}) \times \mathbb{P}(\mathcal{A})$ be a place, and let σ be a trace. With respect to σ , p is called

- *underfed*, denoted by $\nabla_\sigma(p)$, if and only if $\exists k \in \{1, 2, \dots, |\sigma|\}$ such that $|\{i \mid i \in \{1, 2, \dots, k-1\} \wedge \sigma(i) \in I\}| < |\{i \mid i \in \{1, 2, \dots, k\} \wedge \sigma(i) \in O\}|$
- *overfed*, denoted by $\Delta_\sigma(p)$, if and only if $|\{i \mid i \in \{1, 2, \dots, |\sigma|\} \wedge \sigma(i) \in I\}| > |\{i \mid i \in \{1, 2, \dots, |\sigma|\} \wedge \sigma(i) \in O\}|$,
- *fitting*, denoted by $\square_\sigma(p)$, if and only if not $\nabla_\sigma(p)$ or $\Delta_\sigma(p)$.

Definition 2.4. (Behavior of a Petri net)

We define the *behavior* of the Petri net (A, P) to be the set of traces with respect to which the places in P are fitting, that is $\{\sigma \in \mathcal{T} \mid \forall p \in P: \square_\sigma(p)\}$.

Note that we only allow for behaviors of the form $\langle \blacktriangleright, a_1, a_2, \dots, a_n, \blacksquare \rangle$ (compare Definition 2.1) such that all places are empty at the end of replaying the trace and never have a negative number of tokens. The behavior of the example Petri net in Figure 3 is $\{\langle \blacktriangleright, a, \blacksquare \rangle, \langle \blacktriangleright, b, c, \blacksquare \rangle, \langle \blacktriangleright, c, b, \blacksquare \rangle\}$.

We are often interested in the multisets of traces of the event log, which are fitting, underfed or overfed by certain (sets of) places.

Definition 2.5. (Multisets of Fitting/Underfed/Overfed Traces)

Given a set of places $P \in \mathbb{P}(\mathcal{A}) \times \mathbb{P}(\mathcal{A})$ and an event log L , we define the following functions with respect to a place $p \in P$:

- $\text{fitting}_L(p) = [\sigma \in L \mid \square_\sigma(p)]$ is the multiset of fitting log traces for p
- $\text{underfed}_L(p) = [\sigma \in L \mid \nabla_\sigma(p)]$ is the multiset of underfed log traces for p
- $\text{overfed}_L(p) = [\sigma \in L \mid \Delta_\sigma(p)]$ is the multiset of overfed log traces for p

We extend these functions to a set of places P as follows:

- $\text{fitting}_L(P) = [\sigma \in L \mid \forall p \in P: \square_\sigma(p)] = \bigwedge_{p \in P} \text{fitting}_L(p)$.
- $\text{underfed}_L(P) = [\sigma \in L \mid \exists p \in P: \nabla_\sigma(p)] = \bigcup_{p \in P} \text{underfed}_L(p)$.
- $\text{overfed}_L(P) = [\sigma \in L \mid \exists p \in P: \Delta_\sigma(p)] = \bigcup_{p \in P} \text{overfed}_L(p)$.

A fitness metric can be used to assign a value to a place, indicating how well it fits a given event log.

Definition 2.6. (Measuring Fitness of a Place)

Given an event log L we define a *fitness metric* to be a function $\text{fm}^L(p): \mathbb{P}(\mathcal{A}) \times \mathbb{P}(\mathcal{A}) \rightarrow [0, 1]$, which assigns a fitness score to a place based on L such that 0 represents the lowest achievable fitness, while 1 reflects the highest achievable fitness.

Based on a fitness metric and a threshold we can classify a place as fitting or unfitting with respect to a complete event log rather than a single trace.

An example of such a tree-structured candidate space is shown in Figure 4. Note the incremental structure of the trees, i.e., the increase in distance from the roots corresponds to the increase of input (red edges) and output (blue edges) activities. Each level of the tree contains all possible places than can be created by connecting the corresponding number of activities (excluding \blacktriangleright as an outgoing activity and \blacksquare as an ingoing activity, since such places cannot fit), with the root level consisting of all candidate places that can be build using exactly two transitions.

We define the edges of the trees in such a way, that all candidates are reachable from exactly one root by a unique path (compare Definition 3.1). Thus, candidate traversal according to the tree structure guarantees that all candidates are considered exactly once. Organization of candidates within the same depth and their connections to parent and child candidates is not fixed, but defined by ordering strategies for of ingoing activities ($>_i$) and outgoing activities ($>_o$). With knowledge of these ordering strategies we can deterministically compute the next candidate place to be considered based on the last candidate we evaluated, i.e., based only on the connected activities of the last place. This is very space efficient, since we do not need to keep the whole tree in memory. It also contributes to time efficiency: we do not only avoid evaluation of candidates in skipped subtrees but do not even need to compute and traverse them.

Definition 3.1. (Complete Candidate Tree)

Let A be a set of activities and let $>_i, >_o$ be two total orderings on this set of activities. A *complete candidate tree* is a pair $CT = (N, F)$ with $N = \{(I|O) \mid I \subseteq A \setminus \{\blacksquare\} \wedge O \subseteq A \setminus \{\blacktriangleright\} \wedge I \neq \emptyset \wedge O \neq \emptyset\}$. We have that $F = F_{\text{red}} \cup F_{\text{blue}}$, with

$$F_{\text{red}} = \{((I_1|O_1), (I_2|O_2)) \in N \times N \mid |O_2| = 1 \wedge O_1 = O_2 \\ \wedge \exists a \in I_1 : (I_2 \cup \{a\} = I_1 \wedge \forall a' \in I_2 : a >_i a')\} \text{ (red edges)}$$

$$F_{\text{blue}} = \{((I_1|O_1), (I_2|O_2)) \in N \times N \mid I_1 = I_2 \\ \wedge \exists a \in O_1 : (O_2 \cup \{a\} = O_1 \wedge \forall a' \in O_2 : a >_o a')\} \text{ (blue edges)}.$$

If $((I_1|O_1), (I_2|O_2)) \in F$, we call the candidate $(I_1|O_1)$ the *child* of its *parent* $(I_2|O_2)$.

The runtime of the eST-Miner strongly depends on the number of candidate places skipped during the search for fitting places. In Figure 5, the subset relations between the sets of places relevant to the eST-Miner framework are visualized. To illustrate the effect of cutting off candidate subtrees, the absolute number of places in these sets is shown for two example applications of the algorithm on two different event logs. While the size of the complete candidate space is the same for both event logs (based on the number of activities), the ordering of the candidates within the tree and properties of the event logs themselves result in different sizes for the subset of candidate places to be evaluated.

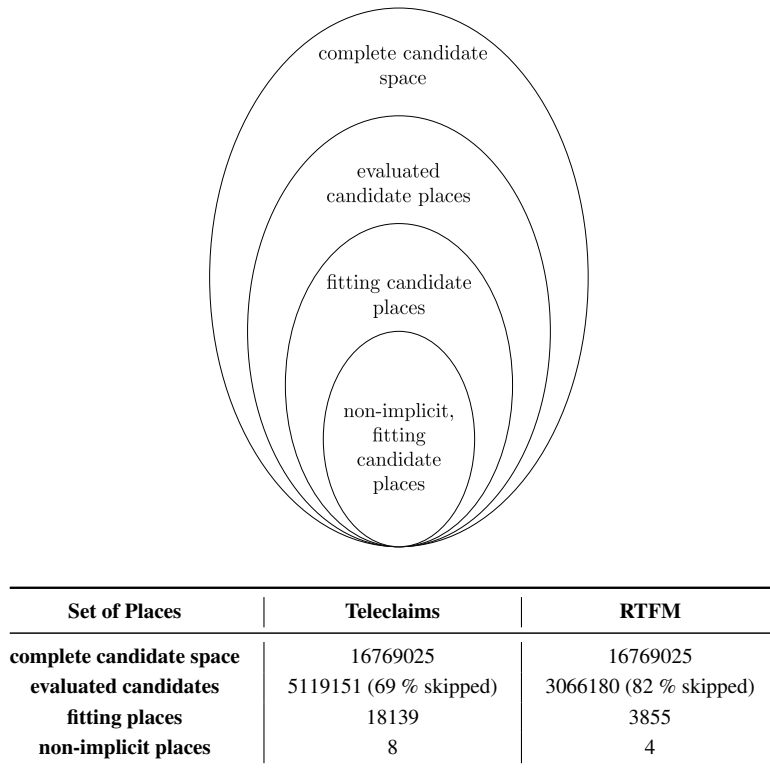


Figure 5. Comparison of the sets of places considered within the eST-Miner framework. To exemplify the impact of cutting off unfitting subtrees we choose the well-known Teleclaims and Road Traffic Fine Management event logs (both have $11 + |\{\blacktriangleright, \blacksquare\}| = 13$ activities) with $\tau = 1.0$ (i.e., requiring all places to be perfectly fitting). The table shows the size relations of the computed sets of places to the complete candidate space (for lexicographical activity orderings $>_i$ and $>_o$ in the complete candidate tree).

4. Problem Explanation and Solution Framework

Basic event log filtering, i.e., simply removing activities or trace variants, can be done easily and efficiently using available tools, e.g., in the ProM framework ([27]). Therefore, it is reasonable to assume that any activities or variants the user considers to be uninteresting, e.g., because of infrequent occurrence, have been removed from the input event log. More advanced filtering approaches aiming to simplify the event log before applying a discovery algorithms exist. However, without in-depth knowledge of the control-flow such filtering is bound to remain either an approximation (e.g., based on directly-follows relations) or computationally expensive (involving at least partial process discovery already). Thus, we do not expect such filtering to be applied beforehand but instead the proposed algorithm aims to incorporate advanced noise handling into its discovery process, where the input parameter τ helps to distinguish between relevant behavior and deviations.

We differentiate between behavior with a *well-defined* control-flow and *chaotic* behavior without a clear positioning within the control-flow. Well-defined behavior should be represented in our discov-

ered Petri net, even if it occurs only infrequently. Chaotic and infrequent behavior constitutes *noise* or uncommon deviations and should be excluded from the returned model. However, chaotic and frequent behavior indicates a chaotic control-flow and one can argue that this should be made visible within the returned model.

The original eST-Miner evaluates place candidates to be fitting if they can replay a fraction of traces based on the threshold τ . All such fitting places are inserted into the resulting Petri net by simply attaching them to the corresponding uniquely labeled transitions. This approach can result in models that do not meet the user's expectations with respect to fitness, partly because infrequent activities are prone to end up in deadlocking constructs. We will use the small example shown in Figure 6 to demonstrate these problems and motivate our two-fold solution approach.

Motivating the Improved Fitness Evaluation

The eST-Miner variants existing so far evaluate the fitness of a place based on the fraction of log traces it can replay. Places that are unable to replay only a few traces are likely to pass the threshold defined by τ . Places that hinder replay of infrequent activities are hardly penalized by this strategy, since blocking of such activities does not significantly lower the fraction of replayable traces. Therefore, it is likely that returned models include places that dead-lock infrequent activities, no matter how well-defined their control-flow is. We illustrate this issue using the example in Figure 6.

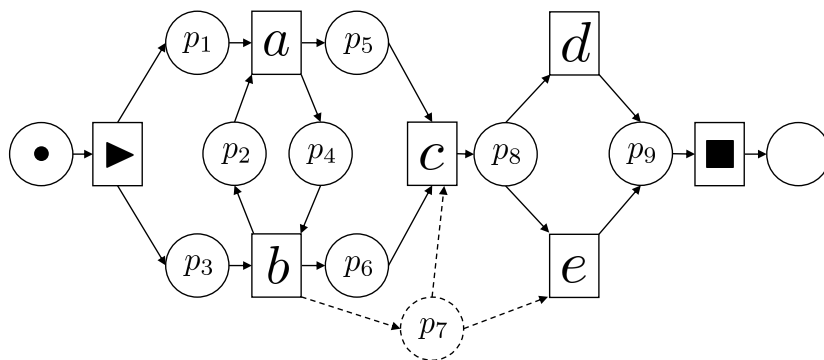


Figure 6. To exemplify the problems addressed in this work we use the Petri net above together with the event log $[\langle \blacktriangleright, a, b, c, d, \blacksquare \rangle^{35}, \langle \blacktriangleright, a, b, c, e, \blacksquare \rangle^5, \langle \blacktriangleright, b, a, c, d, \blacksquare \rangle^{55}, \langle \blacktriangleright, b, a, c, e, \blacksquare \rangle^5]$. One issue is the potential insertion of p_7 instead of the more desirable place p_6 . Another problem is posed by the interaction between p_2 and p_4 .

Consider the given example event log and the place $p_7 = (b|c, e)$ in the Petri net. This place can replay all traces in the event log that do not include the infrequent activity e , i.e., a fraction of 0.9 of all traces. Inserting this place into the Petri net would block e from being executed completely. However, despite occurring only infrequently, activity e exhibits a well-defined control-flow: whenever it occurs in a trace, it replaces execution of activity d after c and before \blacksquare . The place p_6 , which can perfectly replay the event log (i.e., replays a fraction of 1.0 of all traces), is a much better choice but would be removed as implicit after adding p_7 .

In Section 5, we aim to tackle this problem by introducing a new metric to evaluate the fitness of a place. This strategy maintains a high fitness score for places that adequately represent the control-flow behavior of all their connected transitions (e.g., p_6) while places that block too many traces for any of their connected transitions are assigned a low fitness value (e.g., p_7). Additionally, the new metric is defined in such a way that the eST-Miner can still use the evaluation results to improve efficiency by skipping parts of the candidate space.

Motivating Place Selection

When a candidate place is evaluated to be fitting based on L and τ , existing variants of the eST-Miner simply insert the place into the Petri net by connecting it to its uniquely labeled ingoing and outgoing transitions. The resulting Petri net can replay exactly the subset of log traces in the intersection of the traces replayable by all inserted places. This may result in Petri nets that can replay a fraction of traces significantly lower than τ , despite each single place satisfying the threshold. We illustrate the issue using the simple example in Figure 6.

Consider the example event log and the candidate places p_1 to p_6 . All of these places can replay at least a fraction of 0.4 traces in the event log and thus the original eST-Miner would insert them into the Petri net for any threshold $\tau \leq 0.4$. However, the resulting Petri net would not be able to replay any trace at all: the places p_2 and p_3 will block any execution of activities a and b . Two viable solutions exist to obtain a more reasonable model, with the better choice depending on the user's requirements. The first variant, visualized in Figure 7, would be to not include neither p_2 nor p_4 and allow a behavior where a and b are executed in parallel. Alternatively, one can focus on the most frequent behavior and

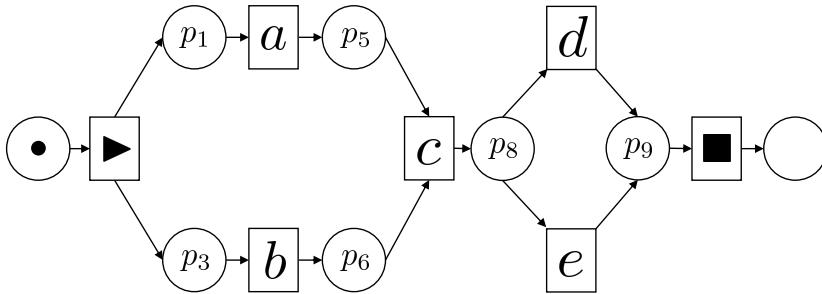


Figure 7. Consider the event log $[\langle \blacktriangleright, a, b, c, d, \blacksquare \rangle^{35}, \langle \blacktriangleright, a, b, c, e, \blacksquare \rangle^5, \langle \blacktriangleright, b, a, c, d, \blacksquare \rangle^{55}, \langle \blacktriangleright, b, a, c, e, \blacksquare \rangle^5]$. The Petri net above is able to perfectly replay all traces in the event log.

insert only p_2 , which would result in the removal of the then implicit places p_1 and p_6 . This second option is illustrated in Figure 8. Based on the low value of the user-definable parameter τ chosen for this example, it would be reasonable to assume the user to be interested in the second option.

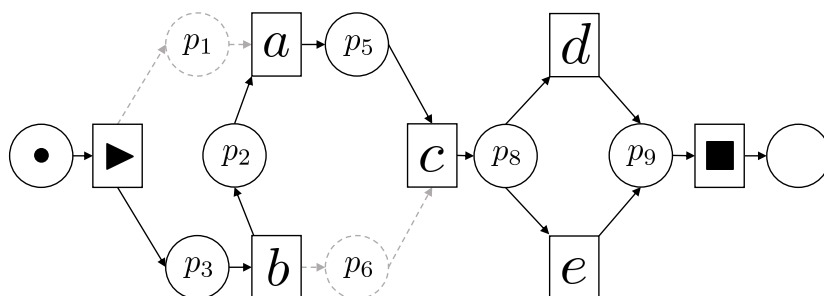


Figure 8. Consider the event log $[\langle \blacktriangleright, a, b, c, d, \blacksquare \rangle^{35}, \langle \blacktriangleright, a, b, c, e, \blacksquare \rangle^5, \langle \blacktriangleright, b, a, c, d, \blacksquare \rangle^{55}, \langle \blacktriangleright, b, a, c, e, \blacksquare \rangle^5]$. The Petri net above (implicit places marked with gray, dashed lines) is able to replay the two trace variants $\langle \blacktriangleright, b, a, c, d, \blacksquare \rangle^{55}$ and $\langle \blacktriangleright, b, a, c, e, \blacksquare \rangle^5$, which constitute a fraction of 0.6 of the input event log.

Overview of the Algorithmic Framework

This work introduces an algorithmic framework extending the eST-Miner with the goal to guarantee minimal in the returned model. To this end, we propose two adaptations of the algorithm which address the two different causes for deadlocks described above. The fitness metric explored in Section 5 refines the evaluation of places connected to rarely occurring activities (e.g., p_7 in Figure 6) to enhance the handling of infrequent behavior. To prevent deadlocks stemming from interactions of places (e.g., p_2 and p_4 in Figure 6), we replace the straightforward place insertion of the eST-Miner with a strategy preventing such structures. This new place insertion strategy is detailed in Sections 6 and 7. The goal is to select a subset of fitting places such that the returned Petri net is guaranteed to replay at least a fraction of τ traces in the event log. At the same time, we aim to maximize simplicity and precision of the model.

The newly introduced place selection strategy focuses on guaranteeing global fitness of the returned Petri net. As illustrated before, places that maintain high global fitness may still have a devastating effect on the fitness of single activities. Conclusively, the proposed fitness metric and the proposed selection technique complement each other but can also be applied independently.

The proposed algorithm is a variant of the eST-Miner and extends the eST-Miner framework by adding and adapting certain submethods. A high-level overview of the framework, including our proposed extensions, is given in Figure 9 and described in the following. Details on the extensions will be provided in the corresponding sections.

Pre-Processing: We expect the input event log L to be already pre-processed in the sense that all trace variants and activities that are uninteresting to the user have been removed. As the only additional pre-processing steps we add artificial start and end activities (\blacktriangleright and \blacksquare) to all traces in the event log and initialize the output model N as a Petri net with one labeled transition for each activity in the input event log (including \blacktriangleright and \blacksquare) and no places except for a marked start place ($\emptyset | \blacktriangleright$) and a final place ($\blacksquare | \emptyset$).

Main Method: The eST-Miner traverses the complete candidate tree (Candidate Traversal) and generates place candidates one by one, which are subsequently evaluated. It uses information on

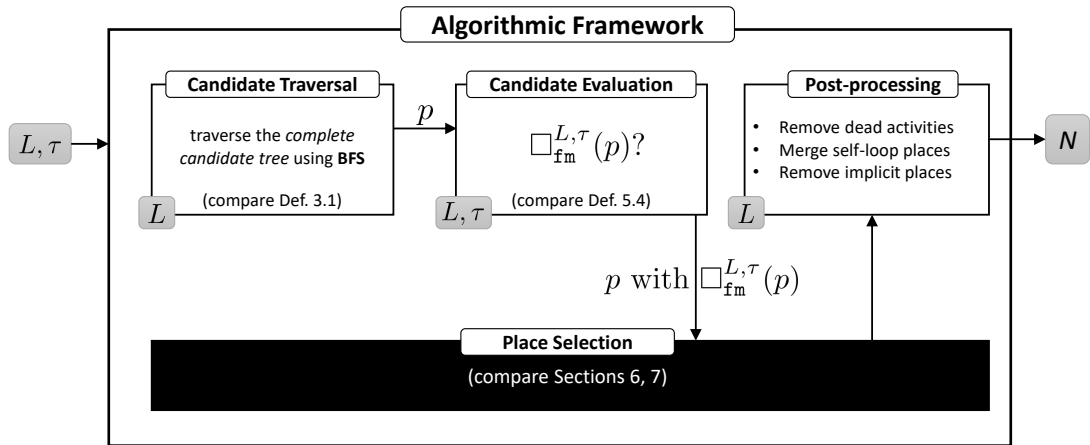


Figure 9. High-level overview of the proposed algorithmic framework. The newly introduced place selection submethod (represented as a black box) is described in detail in Sections 6 and 7.

the fitness evaluation results to skip subtrees while guaranteeing that all fitting place candidates are visited (details provided in Section 5). Different traversal strategies are possible, e.g. Depth-First-Search, Breadth-First-Search or guided by heuristics. It is also possible to limit the depth of tree traversal, improving computation time while losing the option to discover any place below that depth. The extension proposed in this paper, with details provided in Sections 6 and 7, requires a Breadth-First-Search traversal strategy and allows limiting the traversal depth.

Every traversed place candidate is evaluated one by one (Candidate Evaluation) to measure how fitting they are with respect to the event log L and the noise threshold τ . Different fitness metrics can be used here. Section 5 provides further details and introduces a new fitness metric to mitigate the previously described issues stemming from places blocking infrequent activities.

The place selection subroutine (Place Selection) following place evaluation is introduced in detail in Sections 6 and 7. When using the original eST-Miner, places that are determined to be fitting are immediately added to the Petri net. As described before, this may result in deadlocks and unnecessarily complex results. This work explores a strategy to select a subset of places out of the set of fitting places such that these issues are prevented. The selected places are added to the Petri net by connecting them to their corresponding uniquely labeled transitions.

Post-Processing: After the selected fitting places have been added, we apply a set of post-processing steps. The proposed place selection strategy may result in certain activities to be no longer included in the replayable part of the event log. The corresponding transitions are removed from the Petri net (details are provided in Section 6).

In the next post-processing step we remove implicit places. We have two approaches at our disposal. The first option is to solve optimization problems to identify implicit places on the structure of the Petri net, as proposed for the original eST-Miner. This approach guarantees that all implicit places are removed and none are removed incorrectly, but is computationally expensive. The second approach replays the event log to compare the markings of the places and uses this information to

compute non-minimal regions, corresponding to implicit places ([26]). While it is much faster, for correct and complete implicit place identification certain requirements must be satisfied, e.g. sufficient similarity between the event log and behavior of the Petri net as well as guaranteed inclusion of certain places in the Petri net. Adaptation of this approach to the context of this work is out of scope, therefore, we use the first implicit place removal variant in the context of this work.

One of the advantages of the eST-Miner is its ability to discover places with self-loops, which can be used to model complex control-flow structures. However, due to the limitations of using uniquely labeled transitions (i.e., no silent or duplicate transitions) self-loops (and loops in general) are also discovered to allow for activities (or submodels) to be skipped. If the tree depth is limited, it is possible that a place with several self-looping transitions is not discovered because it is too low in the tree structure. As an example for such a place consider $p = (I \cup \{a_1, a_2\} | O \cup \{a_1, a_2\})$, where a_1 and a_2 are self-looping. Such a place can be split into a set of smaller places that are positioned closer to the roots of the tree-structured candidate space and therefore have been added to the Petri net. For the example place p , this would be the places $p_1 = (I \cup \{a_1\} | O \cup \{a_1\})$ and $p_2 = (I \cup \{a_2\} | O \cup \{a_2\})$. To simplify the resulting Petri net, such small self-looping places are identified and merged without impact on the Petri net's behavior, i.e., p_1 and p_2 would be replaced by p .

5. Fitness Evaluation and Noise Filtering

The eST-Miner considers all possible candidate places based on the activities in the event log. Therefore, in the following, we consider only places whose sets of ingoing and outgoing activities occur in the corresponding event log at least once. The number of such possible places is exponential in the number of observed unique activities, and therefore the approach aims to increase efficiency by skipping uninteresting sets of candidate places, while still discovering all places that are considered *fitting*. This is enabled by cutting off subtrees in the complete candidate tree (Definition 3.1) based on *monotonicity properties* of place candidates that are evaluated to be *unfitting*.

Theorem 5.1. (Monotonicity Properties, cf. [22])

Consider two places $p_1 = (I_1 | O_1)$ and $p_2 = (I_2 | O_2)$. Then the following holds:

- $I_1 \supseteq I_2 \wedge O_1 \subseteq O_2 \implies \text{underfed}_L(p_1) \subseteq \text{underfed}_L(p_2)$
- $I_1 \subseteq I_2 \wedge O_1 \supseteq O_2 \implies \text{overfed}_L(p_1) \subseteq \text{overfed}_L(p_2)$

Consider any place candidate p in the complete candidate tree (Definition 3.1). By construction, the tree structure guarantees that for every descendant p_{blue} of p reachable via a path of purely blue edges we have that $\text{underfed}_L(p) \subseteq \text{underfed}_L(p_{blue})$ and, respectively, for every descendant p_{red} of p reachable via purely red edges, we have that $\text{overfed}_L(p) \subseteq \text{overfed}_L(p_{red})$. Combining this property with a suitable fitness metric allows us to cut off subtrees consisting of only unfitting candidate places based on the replay result of the root candidate place. In [22], two such fitness metrics have been proposed, in the following called *absolute fitness* and *relative fitness*. In an attempt to improve handling of infrequent activities, this work introduces *aggregated fitness*.

Before introducing the fitness metrics, we define the multiset of traces in an event log which are activated by a given set of activities.

Definition 5.2. (Activated Traces)

Given an event log L and a set of activities $A \subseteq \mathcal{A}$, we define the multiset of traces *activated* by A as $\text{act}_L(A) = [\sigma \in L \mid \exists i \in \mathbb{N}: \sigma(i) \in A]$.

We say that a place activates a trace if its connected activities activate the trace.

Definition 5.3. (Fitness Metrics (compare [22]))

Let L be an event log and let $p = (I \mid O)$ be a place. We define three different fitness metrics of the place p with respect to L .

$$\begin{aligned} \text{absolute fitness: } \text{fm}_{\text{abs}}^L(p) &= \frac{|\text{fitting}_L(p)|}{|L|} \\ \text{relative fitness: } \text{fm}_{\text{rel}}^L(p) &= \frac{|\text{act}_L(I \cup O) \uparrow \text{fitting}_L(p)|}{|\text{act}_L(I \cup O)|} \\ \text{aggregated fitness: } \text{fm}_{\text{agg}}^L(p) &= \min_{a \in (I \cup O)} \left(\frac{|\text{act}_L(\{a\}) \uparrow \text{fitting}_L(p)|}{|\text{act}_L(\{a\})|} \right) \end{aligned}$$

All three metrics return values between 0 (low fitness) and 1 (high fitness).

Aggregated fitness as introduced in Definition 5.3 returns the minimal fitness computed for each individual transition of the place. Other aggregation methods such as average, mean or harmonic mean may yield interesting fitness results, as they also penalize places that have extremely low fitness for one or more of their connected transitions. *However, to maintain the eST-Miners efficiency we require the chosen metric to allow for cutting off subtrees by exploiting the monotonicity properties of the places (Definition 5.1), i.e., the metric has to guarantee that there are no fitting places in the skipped subtrees of the complete candidate tree.* In the following, we show that the proposed *aggregated fitness* can satisfy this requirement.

To enable exploitation of the monotonicity results for skipping candidate subtrees while employing the noise threshold τ to handle infrequent behavior, we extend the notions of fitting, underfed and overfed (compare Definition 2.3) from single traces to the whole event log in a suitable way:

- A place is considered *fitting* with respect to the log and the noise threshold τ if the value returned by the fitness metric used is at least as large as τ . A fitting place cannot simultaneously be underfed, overfed or unfitting.
- A place that is unfitting, i.e., not fitting, can be further classified as *underfed* and/or *overfed*. If a place is *underfed* (respectively *overfed*) with respect to the log and noise threshold τ , we guarantee that all its descendants in the complete candidate tree reachable via blue edges (respectively red edges) are also underfed (respectively overfed). A place can be underfed and overfed at the same time.
- In contrast to the trace level, a place can be *unfitting* with respect to an event log without necessarily satisfying the requirements to be underfed or overfed. Such a place cannot be used to skip parts of the candidate space.

Figure 10 illustrates the fitness status a place can have with respect to an event log and a noise threshold. As an example, consider the event log $L = [\langle \blacktriangleright, a, b, d, \blacksquare \rangle^{60}, \langle \blacktriangleright, a, c, d, \blacksquare \rangle^{40}]$ and noise threshold $\tau = 0.5$. For all fitness metrics discussed in this paper, with respect to L and τ the place $p_1 = (a|b)$ is fitting, $p_2 = (c|d)$ is underfired, $p_3 = (a|c)$ is overfired, and $p_4 = (d|a)$ is underfired as well as overfired.

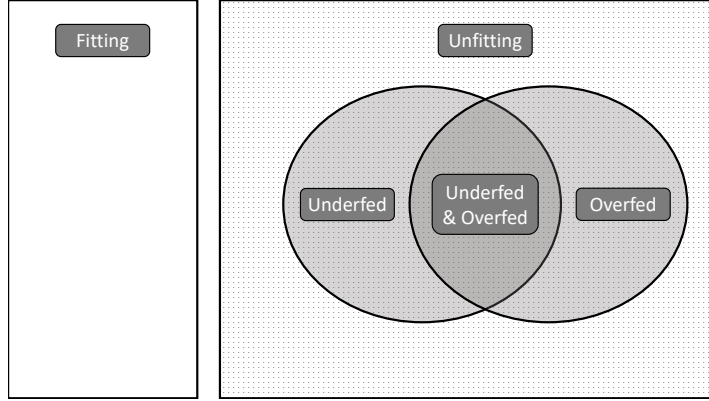


Figure 10. Illustrating the fitness status a place can have with respect to an event log and noise threshold. A place can either be fitting or unfitting. If it is unfitting, it may be underfired, overfired or both, enabling the skipping of derived candidate places. If the place is simply unfitting without being underfired or overfired, no candidates can be skipped based on it.

Definition 5.4. (Underfired/Overfired/Fitting Places with Respect to an Event Log (compare [22]))

With respect to an event log L and a noise parameter $\tau \in [0, 1]$ we define a place $p = (I|O)$ to be *underfired*, *overfired*, *fitting* or *unfitting* based on the fitness metric used.

For *absolute fitness*, we call p

- *fitting*, denoted by $\square_{abs}^{L,\tau}(p)$, if and only if $\text{fm}_{abs}^L(p) = \frac{|\text{fitting}_L(p)|}{|L|} \geq \tau$,
- *unfitting*, denoted by $\boxtimes_{abs}^{L,\tau}(p)$, if not $\square_{abs}^{L,\tau}(p)$.
An unfitting place can be classified further as

- *underfired*, denoted by $\nabla_{abs}^{L,\tau}(p)$, if and only if $\frac{|\text{underfired}_L(p)|}{|L|} > 1 - \tau$,
- *overfired*, denoted by $\triangle_{abs}^{L,\tau}(p)$, if and only if $\frac{|\text{overfired}_L(p)|}{|L|} > 1 - \tau$.

For *relative fitness*, we call p

- *fitting*, denoted by $\square_{rel}^{L,\tau}(p)$, if and only if $\text{fm}_{rel}^L(p) = \frac{|\text{act}_L(I \cup O) \cap \text{fitting}_L(p)|}{|\text{act}_L(I \cup O)|} \geq \tau$,
- *unfitting*, denoted by $\boxtimes_{rel}^{L,\tau}(p)$, if not $\square_{rel}^{L,\tau}(p)$.
An unfitting place can be classified further as

- *underfed*, denoted by $\nabla_{rel}^{L,\tau}(p)$, if and only if $\frac{|\text{act}_L(I \cup O) \uparrow \text{underfed}_L(p)|}{|\text{act}_L(I \cup O)|} > 1 - \tau$,
- *overfed*, denoted by $\Delta_{rel}^{L,\tau}(p)$, if and only if $\frac{|\text{act}_L(I \cup O) \uparrow \text{overfed}_L(p)|}{|\text{act}_L(I \cup O)|} > 1 - \tau$.

For *aggregated fitness*, we call p

- *fitting*, denoted by $\square_{agg}^{L,\tau}(p)$, if and only if $\text{fm}_{agg}^L(p) = \min_{a \in (I \cup O)} \left(\frac{|\text{act}_L(\{a\}) \uparrow \text{fitting}_L(p)|}{|\text{act}_L(\{a\})|} \right) \geq \tau$,
 - *unfitting*, denoted by $\boxtimes_{agg}^{L,\tau}(p)$, if not $\square_{agg}^{L,\tau}(p)$.
- An unfitting place can be classified further as

- *underfed*, denoted by $\nabla_{agg}^{L,\tau}(p)$, if and only if $\exists a \in I \cup O : \frac{|\text{act}_L(\{a\}) \uparrow \text{underfed}_L(p)|}{|\text{act}_L(\{a\})|} > 1 - \tau$,
- *overfed*, denoted by $\Delta_{agg}^{L,\tau}(p)$, if and only if $\exists a \in I \cup O : \frac{|\text{act}_L(\{a\}) \uparrow \text{overfed}_L(p)|}{|\text{act}_L(\{a\})|} > 1 - \tau$.

Definition 5.4 ensures that a place determined to be underfed, overfed or unfitting with respect to an event log L , based on a noise parameter τ and a fitness metric fm , cannot be fitting at the same time. Note that it also allows for a place to be underfed and overfed at the same time, given that sufficiently many traces validate the necessary requirements, or to be unfitting without being neither underfed nor overfed.

A prerequisite for the eST-Miner to skip parts of the candidate space is the guarantee, that if a place is determined to be underfed (overfed), the same is guaranteed to be true for its blue (red) descendants in the complete candidate tree.

Lemma 5.5. (Monotonicity of Fitness Metrics)

Consider an event log L and a noise threshold $\tau \in [0, 1]$.

For two places $p = (I|O)$ and $p' = (I|O')$ with $O \subseteq O'$ the following implications hold:

$$\nabla_{abs}^{L,\tau}(p) \implies \nabla_{abs}^{L,\tau}(p'), \quad (1)$$

$$\nabla_{rel}^{L,\tau}(p) \implies \nabla_{rel}^{L,\tau}(p'), \quad (2)$$

$$\nabla_{agg}^{L,\tau}(p) \implies \nabla_{agg}^{L,\tau}(p'), \quad (3)$$

For two places $p = (I|O)$ and $p'' = (I''|O)$ with $I \subseteq I''$ the following implications hold:

$$\Delta_{abs}^{L,\tau}(p) \implies \Delta_{abs}^{L,\tau}(p''), \quad (4)$$

$$\Delta_{rel}^{L,\tau}(p) \implies \Delta_{rel}^{L,\tau}(p''), \quad (5)$$

$$\Delta_{agg}^{L,\tau}(p) \implies \Delta_{agg}^{L,\tau}(p''). \quad (6)$$

Proof:

Implications 1, 2, 4 and 5 have already been shown in [22]. We proceed with showing Implications 3 and 6:

First, assume that $\nabla_{agg}^{L,\tau}(p)$. Then, by definition, there exists some activity $a \in I \cup O$ such that $\frac{|\text{act}_L(\{a\}) \uplus \text{underfed}_L(p)|}{|\text{act}_L(\{a\})|} > 1 - \tau$. Because of $O \subseteq O'$ we know that $a \in I \cup O'$. Also, by Theorem 5.1 we have that $\text{underfed}_L(p) \subseteq \text{underfed}_L(p')$. Together, this implies that $\frac{|\text{act}_L(\{a\}) \uplus \text{underfed}_L(p')|}{|\text{act}_L(\{a\})|} \geq \frac{|\text{act}_L(\{a\}) \uplus \text{underfed}_L(p)|}{|\text{act}_L(\{a\})|} > 1 - \tau$, and thus by definition $\nabla_{agg}^{L,\tau}(p')$.

Now, assume that $\Delta_{agg}^{L,\tau}(p)$. Then, by definition, there exists an activity $a \in I \cup O$ such that $\frac{|\text{act}_L(\{a\}) \uplus \text{overfed}_L(p)|}{|\text{act}_L(\{a\})|} > 1 - \tau$. Because of $I \subseteq I''$ we know that $a \in I'' \cup O$. By Theorem 5.1 we have that $\text{overfed}_L(p) \subseteq \text{overfed}_L(p'')$. Together, this implies that $\frac{|\text{act}_L(\{a\}) \uplus \text{overfed}_L(p'')|}{|\text{act}_L(\{a\})|} \geq \frac{|\text{act}_L(\{a\}) \uplus \text{overfed}_L(p)|}{|\text{act}_L(\{a\})|} > 1 - \tau$, and thus by definition $\Delta_{agg}^{L,\tau}(p'')$. \square

We have shown that the monotonicity properties of the newly introduced *aggregated fitness* enable the same efficiency optimizations by skipping candidate subtrees as the absolute and relative fitness. Thus, this metric can be easily integrated into the eST-Miners framework. To compare the impact on the place fitness evaluation, we continue to investigate relationships between these fitness metrics.

Lemma 5.6. (Relationships Between Fitness Metrics)

Let L be an event log and let $p = (I|O)$ be a place. Then the following holds:

$$\text{fm}_{rel}^L(p) \leq \text{fm}_{abs}^L(p).$$

Proof:

With respect to the place p , we can partition the event log L into the following disjunct multisets of traces:

$$L_{\checkmark}^{\square} = \text{fitting}_L(p) \uplus \text{act}_L(I \cup O), \text{ the multiset of fitting, activated traces.}$$

$$L_{\checkmark}^{\boxtimes} = (\text{underfed}_L(p) \uplus \text{overfed}_L(p)) \uplus \text{act}_L(I \cup O), \text{ the multiset of unfitting, activated traces.}$$

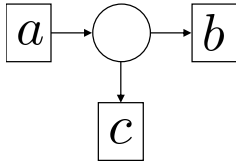
$$L_{\times} = L \setminus \text{act}_L(I \cup O), \text{ the multiset of non-activated traces.}$$

Note that $|L_{\checkmark}^{\square}| + |L_{\checkmark}^{\boxtimes}| > 0$, since we consider only activities contained in L . In the following, we use these sets to rewrite absolute and relative fitness and show the claimed relation between them:

$$\begin{aligned} \text{fm}_{rel}^L(p) &\leq \text{fm}_{abs}^L(p) \\ \Leftrightarrow \frac{|L_{\checkmark}^{\square}|}{|L_{\checkmark}^{\square}| + |L_{\checkmark}^{\boxtimes}|} &\leq \frac{|L_{\checkmark}^{\square}| + |L_{\times}|}{|L_{\checkmark}^{\square}| + |L_{\checkmark}^{\boxtimes}| + |L_{\times}|} \\ \Leftrightarrow |L_{\checkmark}^{\square}| \cdot (|L_{\checkmark}^{\square}| + |L_{\checkmark}^{\boxtimes}| + |L_{\times}|) &\leq (|L_{\checkmark}^{\square}| + |L_{\times}|) \cdot (|L_{\checkmark}^{\square}| + |L_{\checkmark}^{\boxtimes}|) \\ \Leftrightarrow |L_{\checkmark}^{\square}|^2 + |L_{\checkmark}^{\square}| \cdot |L_{\checkmark}^{\boxtimes}| + |L_{\checkmark}^{\square}| \cdot |L_{\times}| &\leq |L_{\checkmark}^{\square}|^2 + |L_{\times}| \cdot |L_{\checkmark}^{\square}| + |L_{\checkmark}^{\square}| \cdot |L_{\checkmark}^{\boxtimes}| + |L_{\times}| \cdot |L_{\checkmark}^{\boxtimes}| \\ \Leftrightarrow 0 &\leq |L_{\times}| \cdot |L_{\checkmark}^{\boxtimes}| \end{aligned}$$

\square

We have shown that relative fitness is at least as strict as absolute fitness. Therefore, using relative fitness instead of absolute fitness during candidate place evaluation guarantees the discovered places to be at least as fitting. Unfortunately, no similar relation holds between $\text{fm}_{agg}^L(p)$ and $\text{fm}_{rel}^L(p)$ as illustrated by the example in Figure 11. Consider the given place p and event log L_1 : we have that $\text{fm}_{agg}^{L_1}(p) = \min(\frac{90}{90}, \frac{0}{10}) = 0$, which is strictly smaller than $\text{fm}_{rel}^{L_1}(p) = \frac{90}{100}$. However, considering the same place p and the event log L_2 , we have that $\text{fm}_{agg}^{L_2}(p) = \min(\frac{33}{33}, \frac{33}{66}, \frac{33}{66}) = \frac{1}{2}$ is strictly larger than $\text{fm}_{rel}^{L_2}(p) = \frac{33}{99} = \frac{1}{3}$.



$$L_1 = [\langle a, b \rangle^{90}, \langle x, y \rangle^{20}, \langle c \rangle^{10}]$$

$$L_2 = [\langle a, b, a, c \rangle^{33}, \langle x \rangle^1, \langle b \rangle^{33}, \langle c \rangle^{33}]$$

Figure 11. Traces in L_1 and L_2 which are unfitting with respect to the place $p = (a|b, c)$ are marked in red, while traces not activated are colored gray. For L_1 we have that $\text{fm}_{agg}^{L_1}(p) < \text{fm}_{rel}^{L_1}(p)$, while for L_2 we have that $\text{fm}_{agg}^{L_2}(p) > \text{fm}_{rel}^{L_2}(p)$.

To obtain a metric that guarantees to satisfy a given fitness threshold τ with respect to all three fitness metrics discussed, we define *combined fitness* as a final fitness metric. Combined fitness simply takes the minimum of all three fitness metrics and therefore inherits their monotonicity properties, i.e., when using it to skip parts of the candidate space we maintain the guarantee to not skip any fitting place candidate.

Definition 5.7. (Combined Fitness of a Place)

Let L be an event log and let $p = (I|O)$ be a place. We define the *combined fitness* of the place p with respect to L as $\text{fm}_{comb}^L(p) = \min(\text{fm}_{abs}^L(p), \text{fm}_{rel}^L(p), \text{fm}_{agg}^L(p))$.

Combined fitness is rather restrictive, mostly due to the newly introduced aggregated fitness. More forgiving aggregation function than the minimum, e.g., such as average, mean or harmonic mean, would be interesting to investigate as an alternative. Unfortunately, such aggregations would not allow for the skipping of candidate subtrees in the esT-Miners complete candidate tree, since they do not provide the same monotonicity properties. For example, consider the place $p = (a|b, c)$ and the event log $L = [\langle \blacktriangleright, a, b, b, \blacksquare \rangle^1, \langle \blacktriangleright, a, c, \blacksquare \rangle^1, \langle \blacktriangleright, a, d, \blacksquare \rangle^1]$. The aggregated fitness of p as defined is $\text{fm}_{agg}^L(p) = \min(\frac{2}{3}, \frac{0}{1}, \frac{1}{1}) = 0$ and p would be considered underfitted because of b , allowing us to skip its blue subtree. When taking the average instead of the minimum, the score would be $\text{average}(\frac{2}{3}, \frac{0}{1}, \frac{1}{1}) \approx 0.55$. Consider now the place $p' = (a|b, c, d)$ constructed from p by adding the outgoing activity d . The aggregated fitness of p' is $\text{fm}_{agg}^L(p') = \min(\frac{2}{3}, \frac{0}{1}, \frac{1}{1}, \frac{1}{1}) = 0$ and p' would also be underfitted, as expected. However, when taking the average instead of minimum, the score would be $\text{average}(\frac{2}{3}, \frac{0}{1}, \frac{1}{1}, \frac{1}{1}) \approx 0.66$. This example clearly illustrates that the monotonicity properties necessary to skip subtrees without losing guarantees do not hold for such aggregation functions.

The *combined fitness* is the strictest fitness metric introduced in this work and therefore guarantees that any (set of) places satisfying a threshold τ with respect to combined fitness also satisfies τ with respect to absolute, relative and aggregated fitness. We can still choose to be less restrictive by lowering the threshold τ . Note that due to Lemma 5.6 we do not need to compute absolute fitness in the implementation of combined fitness. In Section 8 we apply the proposed eST-Miner variant with *combined fitness* as well as *relative fitness* as a fitness metric to various event logs to evaluate their impact on real-life data.

6. Place Selection

The eST-Miner evaluates all candidate places and discovers a set of places fitting the input event log based on the noise threshold τ and the chosen fitness metric. As illustrated by the simple example in Figure 6, simply adding all fitting places to a Petri net indiscriminately may result in deadlocks and unnecessary complexity. In this section, we propose an approach aiming to mitigate this problem by selecting a suitable subset of places.

To motivate our strategy, we first discuss a more complex example. Consider the event log L and the set of places p_1 to p_8 in Figure 12. For each of the three fitness metrics introduced in Definition 5.3, all places in this (incomplete) subset of candidate places are *fitting* with respect to L and $\tau = 0.75$. Inserting all of these places results in the given Petri net N , which can replay only the first trace variant in L , corresponding to 60 % of the traces. The introductory example in Figure 6 illustrates, that the fraction of replayable traces may even decrease to 0. Such a result is undesirable, since it is unnecessarily complex with respect to the behavior it represents, not free of dead parts and likely to disappoint user expectations with respect to fitness. In the following, we explore strategies to return a dead-lock free Petri net that is guaranteed to replay at least a fraction of τ traces in the event log by inserting only a selection of the discovered fitting places.

Consider the set of all fitting places discovered during the place candidate evaluation of the eST-Miner. Selecting an adequate subset of these places, such that also the resulting Petri net as a whole satisfies the noise threshold τ , is non-trivial for a variety of reasons. First of all, the definition of an optimal solution is not straightforward, since several maximal subsets of places satisfying this requirement may exist. These subsets may differ, for example, in size, fraction of replayable traces, place complexity (number of connected activities) or subjective 'interestingness' measures. Figure 13 illustrates all maximal sets of places that can be built from the example places given in Figure 12. These sets are maximal in the sense that adding any of the other places would decrease the number of replayable log traces. Depending on the choice of the minimal fitness threshold τ , the optimal solution is not clear.

Furthermore, even if we have somehow obtained a notion of optimality, first collecting all fitting places and then computing an optimal solution can quickly become unfeasible, both in terms of time complexity and memory requirements. This is due to the huge number of fitting but potentially implicit places discovered by the eST-Miner. Unfortunately, knowledge of which places are contained in the Petri net is required to identify implicit places reliably.

To circumvent the issue of time and space complexity, we combine the eST-Miners sequential place evaluation procedure with a guided greedy place selection approach, which is described in detail

ID	Traces in L	p_1 (▶ a)	p_2 (a c)	p_3 (a b)	p_4 (c e)	p_5 (b e)	p_6 (e ■)	p_7 (b c, d)	p_8 (d, e ■)	N
1	$\langle \blacktriangleright, a, b, c, e, \blacksquare \rangle^{60}$	✓	✓	✓	✓	✓	✓	✓	✓	✓
2	$\langle \blacktriangleright, a, b, d, \blacksquare \rangle^{20}$	✓	✗	✓	✓	✗	✗	✓	✓	✗
3	$\langle \blacktriangleright, a, c, b, e, \blacksquare \rangle^{15}$	✓	✓	✓	✓	✓	✓	✗	✓	✗
4	$\langle \blacktriangleright, a, b, d, e, \blacksquare \rangle^5$	✓	✗	✓	✗	✓	✓	✓	✗	✗

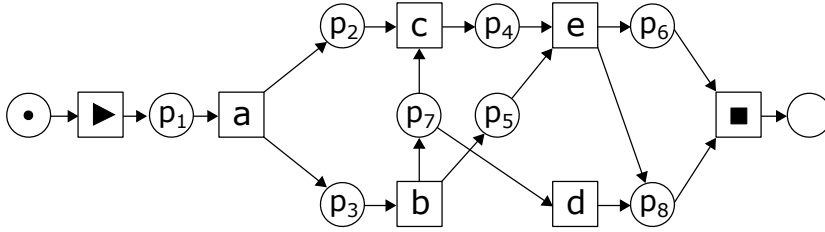


Figure 12. The table indicates for each of the given trace variants and candidate places whether the place can replay that trace variant. The Petri net N is created by inserting all these places and can replay only the first trace variant, i.e., $0.6 \cdot |L| = 60$ traces.

in Subsections 6.1 and 6.2. In the absence of a clear notion of optimality, we propose and investigate several heuristic selection strategies and evaluate their impact on different quality aspects of the returned Petri net. In this paper, we consider fitness, precision, and simplicity as desirable properties.

A model with high fitness can express most of the behavior seen in the event log. High precision means that the model does not allow for a lot of behavior not seen in the event log. Simplicity refers to the general readability and understandability of the model and is very subjective and harder to define. While generality (avoiding overfitting with respect to the sample process executions given in the event log) is desirable, additional information would be required to evaluate it, which is why we consider it outside the scope of this work. For most real-life logs these quality aspects cannot all be perfectly satisfied at the same time (e.g., high fitness often entails low precision and the other way around), and should be balanced according to the user's needs. The concrete metrics used in this work to evaluate quality will be briefly discussed in Section 8. For further details, we refer the reader to [28, 29].

6.1. Place Classification

When making the decision to insert a place into the model, this reduces the possible choices we can make later on: the place constrains the behavior of the model and only places with a sufficiently large intersection of replayable traces can be added to the model at a later point. Consider the example place combinations in Figure 13 with a fitness threshold of $\tau = 0.75$ and assume that the model already contains the places p_1 and p_3 . If the next fitting place we discover is p_7 , and we immediately insert it into the Petri net, we can no longer discover a Petri net including, for example, p_6 , without violating our global fitness constraint. Such choices may prevent us from discovering a more desirable solution. Therefore, we aim to capture the main behavior of the log by using heuristics to postpone,

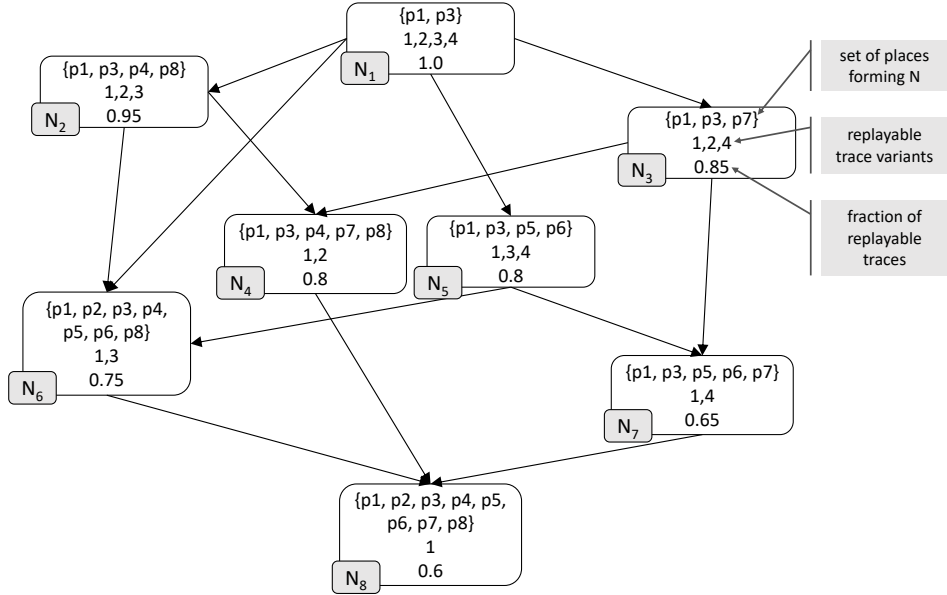


Figure 13. Consider the set of places given in Figure 12. This figure shows all possible combinations of these places such that adding any other place to the corresponding Petri net would decrease the number of replayable log traces. Each set of places, i.e., Petri net, is annotated with the list of trace variants it can replay and the corresponding fraction of log traces. Note that N_8 corresponds to the Petri net shown in Figure 12.

or even disallow, the addition of very restrictive places.

To this end, we introduce a new parameter δ which is our main tool to guide the choice of places while balancing fitness, precision, and simplicity. This δ specifies the largest acceptable reduction in replayable traces when adding a place to the model. Optionally, δ can be adapted for each place individually using an adaption function `adapt` to favor certain places over others, according to the user's preferences. Favored places can be added earlier, despite being rather restrictive, while other places will be added only if they do not constrain the behavior too much. Examples for such strategies are presented in Section 7.

Definition 6.1 formalizes the use of τ , δ and `adapt` to decide for the discovered fitting places, whether they should be added, kept for later re-evaluation or discarded.

Definition 6.1. (Place Classification Using τ , δ and `adapt`)

Consider an event log L over the set of activities $A \in \mathcal{A}$, a set of places $P \subseteq \mathbb{P}(A) \times \mathbb{P}(A)$, and a place $p \in \mathbb{P}(A) \times \mathbb{P}(A)$. We use parameters $\tau \in [0, 1]$ and $\delta \in [0, 1]$, and a function `adapt`: $[0, 1] \times (\mathbb{P}(A) \times \mathbb{P}(A)) \rightarrow [0, 1]$ to categorize p as follows:

$$\begin{aligned} \text{keep}_{L,\tau}(P,p) &= |\text{fitting}_L(P) \cap \text{fitting}_L(p)| \geq \tau \cdot |L| \\ \text{add}_{L,\tau,\delta}(P,p) &= \text{keep}_{L,\tau}(P,p) \\ &\quad \wedge |\text{fitting}_L(P)| - |\text{fitting}_L(P) \cap \text{fitting}_L(p)| \leq \text{adapt}(\delta,p) \cdot |L| \end{aligned}$$

If $\text{keep}_{L,\tau}(P,p)$ does not hold, p will be discarded.

In the following subsection, we give an overview of the complete approach.

6.2. Selection Framework

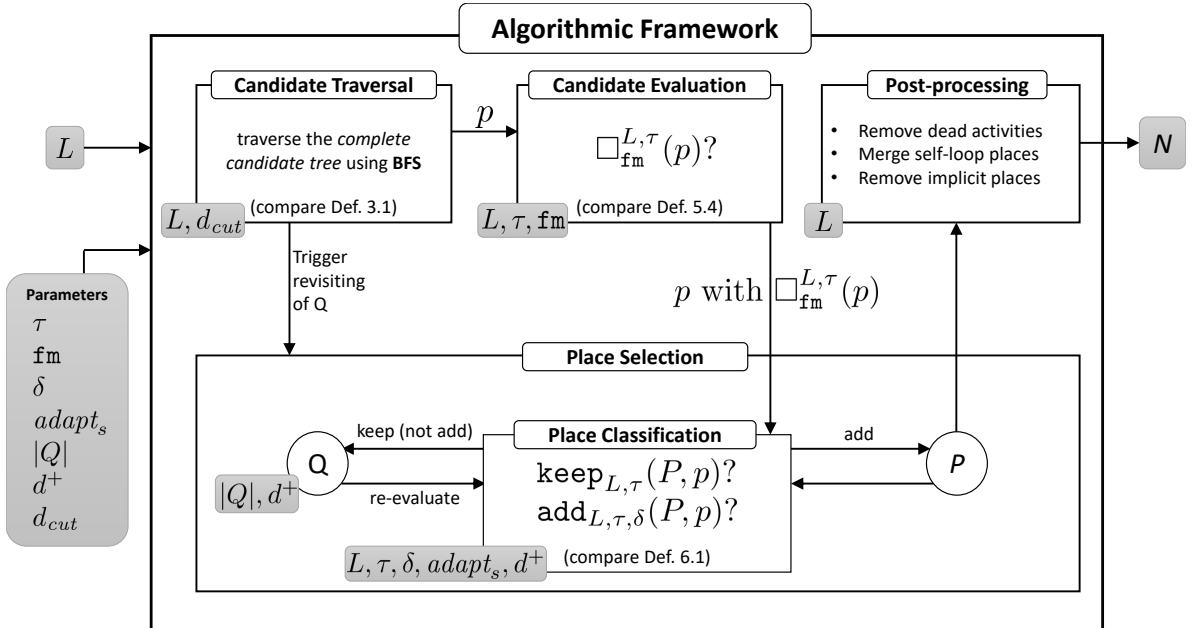


Figure 14. Overview of the presented approach, including input, output, and parameter use.

An overview of our approach, indicating inputs, outputs and use of parameters, is given in Figure 14. Since we consider the simplicity of the model to be a desirable property, we set the eST-Miner to traverse the *complete candidate tree* using BFS rather than DFS. Thus, places with few connected activities are evaluated first and can therefore be inserted into the model at an earlier stage. Furthermore, we limit the traversal depth to places with d_{cut} activities, arguing that places with many transitions are generally not desirable - such places are usually devastating to readability of the Petri net while their constraints can be sufficiently approximated by much simpler places.

After the eST-Miner framework evaluates a candidate place p to be fitting with respect to a threshold τ , we use the *classification functions* given in Definition 6.1 to decide whether the place should immediately be added to the output Petri net, discarded forever or kept for re-evaluation. In the latter case it is added to a queue Q of potential places which is sorted according to how interesting a place is. In our case, we sort first by place simplicity (few transitions are better) and second by the number of replayable log traces. Optionally, the length of Q can be limited, trading an improvement in time and space complexity for potentially lowered model quality.

Whenever the BFS candidate traversal reaches a new level in the *complete candidate tree*, we revisit the potential places queue Q and re-evaluate its places using the classification functions before

proceeding with the traversal of more complex places. This makes sense to promote simplicity in particular together with the delta adaption functions proposed in Section 7, which give preference to places less complex than indicated by the current tree level. After reaching the lowest tree level, the approach can either terminate immediately, or iterate over the potential places queue while artificially increasing the tree depth d^+ times. This can be relevant for delta adaption functions depending on place complexity, as exemplified in Section 7. Here, the artificial tree depth allows for increased leniency also for the most complex places evaluated.

Finally, the resulting Petri net $N = (A, P)$ may contain dead parts: activities which occur only in the subset of log traces that are no longer replayable by N are not guaranteed to be executable at all. Therefore, as a final step, we detect and remove all activities that do not occur in $\text{fitting}_L(P)$ together with their connected arcs. Before returning this Petri net as final output, the eST-Miner framework removes implicit places, and merges self-looping places when applicable (see Section 4).

The approach returns a Petri net N satisfying the following guarantees.

Theorem 6.2. (Guarantees)

Given an event log L over activities A , an adaption function $\text{adapt}: [0, 1] \times (\mathbb{P}(A) \times \mathbb{P}(A)) \rightarrow [0, 1]$ and parameters $\tau \in [0, 1], \delta \in [0, 1], s \in \mathbb{N}, |Q| \in \mathbb{N}, d^+ \in \mathbb{N}, d_{cut} \in \mathbb{N}$, the presented approach computes a Petri net $N = (A', P)$ with $A' \subseteq A$, such that N can replay at least $\tau \cdot |L|$ traces from L and every transition in A' can be fired at least once.

Furthermore, if the length of Q is not limited, and thus a place p is discarded only if it does not satisfy $\text{keep}_{L,A,\tau}(P, p)$, the set of places P is maximal in the sense that no place from the set of evaluated candidate places can be added without violating the fitness constraints imposed by the chosen heuristics.

7. Selection Strategies

As illustrated by the example place combinations in Figure 13, the order of places added can have a significant impact on the selected subset of places and, thus, the behavior of the returned Petri net. The presented framework allows for a wide range of heuristic functions, optimizing the place selection individually towards a variety of possible user interests. Thus, obviously, the examples presented in the following are by far not exhaustive and entirely different choices are possible, but they can serve as a starting point for an investigation of the impact and suitability of our approach.

The *linear* and *sigmoid* delta adaption functions both aim to promote fitness and simplicity, but balance them in different ways. The *constant* and *no delta* delta adaption functions are introduced to be used as a baseline in our experiments, towards which the effect of the other strategies can be compared.

No Delta

As a baseline to compare to, we introduce a function that ignores the parameter δ and simply adds every fitting place to the Petri net as soon as it is discovered. Within the framework, this can be

formalized to

$$\text{adapt}_{noDelta}(\delta, p) = 1.$$

Constant Delta

Trivially, we can choose not to adapt delta at all. We simply add every fitting, non-discarded place that does not reduce the replayable traces from the log by a fraction of more than delta. Formally, this resembles the identity function:

$$\text{adapt}_{constant}(\delta, p) = \delta$$

Linear and Sigmoid Delta Adaption

While optimizing towards fitness as well as simplicity, we can balance the two forces in different ways based on the details of the adaption function. In this work, we aim to investigate the impact of such choices using *linear* and *sigmoid* delta adaption as defined in the following and visualized in Figure 15.

Given a set of activities A , the maximum depth of the complete candidate tree is $d_{max} = 2|A|$. Furthermore, let $d \in [2, 3, \dots, d_{max}]$ be the current depth of the candidate tree traversal. We call $s \in \mathbb{N} \setminus \{0\}$ the *steepness modifier*. Consider a place $p = (I|O)$.

The *linear delta adaption function* computes the adapted δ as follows:

$$\begin{aligned} \text{adapt}_{linear}(\delta, (I|O)) &= \delta \cdot \text{mod}_{linear}((I|O)) \\ &= \delta \cdot \frac{s}{(|I| + |O|)} \cdot \frac{d - (|I| + |O|)}{d_{max} - 2} \end{aligned}$$

We define the *sigmoid delta adaption function* as follows:

$$\begin{aligned} \text{adapt}_{sigmoid}(\delta, (I|O)) &= \delta \cdot \text{mod}_{sigmoid}((I|O)) \\ &= \delta \cdot \left(\frac{2}{1 + \exp\left((-1) \cdot \frac{s}{(|I| + |O|)} \cdot (d - (|I| + |O|))\right)} - 1 \right) \end{aligned}$$

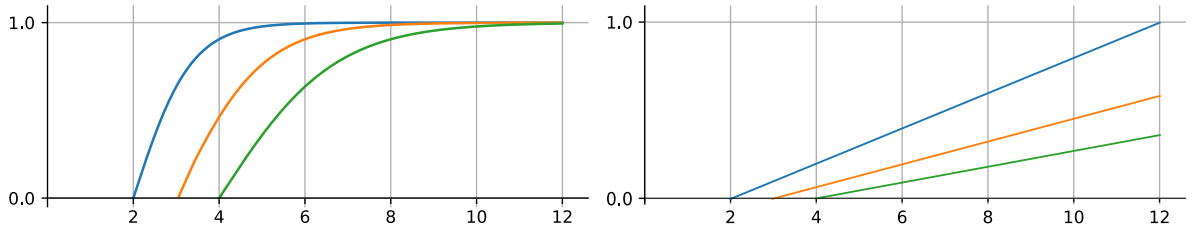


Figure 15. Example behavior of the delta adaption modifiers $\text{mod}_{sigmoid}(\delta)$ (left) and $\text{mod}_{linear}(\delta)$ (right) for three places with 2, 3, and 4 activities, respectively. The x-axis indicates the current tree depth d , with $d_{max} = 12$, while the y-axis indicates the modifier to be multiplied with δ .

Both adaption functions multiply a modifier with the parameter δ . Figure 15 illustrates the behavior of this modifier for three example places of varying complexity. Both, the *linear* and *sigmoid* delta adaption are designed to prefer simple places. When a place originates from the currently traversed level of the *complete candidate tree*, i.e., it is among the most complex places currently available, both functions will evaluate to 0, meaning that only a perfectly fitting place can be added. The simpler the evaluated place is compared to the current tree level, the larger the result of the function and the more unfitting traces are allowed, with δ marking the maximal returnable value. The difference is in the slope of the functions: while the linear function increases linearly with the place complexity, the sigmoid function grows fast in the beginning, but stagnates towards the end. The steepness modifier s controls the intensity of this growth behavior. In general, the linear function becomes uniformly less lenient with increasing place complexity. In contrast, the sigmoid function prefers the simpler places more strongly, while the more complex places are (roughly) equally undesirable.

8. Experimentation and Evaluation

We performed several experiments where we run the proposed algorithm with a wide variation of combinations of possible parameter settings on several event logs with different properties. To investigate the impact of the proposed heuristics, we use a lexicographical ordering of the activities, thus fixing the order of candidate evaluation. The purpose is to focus on the effect of the different parameters, and possibly derive which of them are the most relevant for the discovery of certain models and whether certain (combinations of) settings are preferable.

8.1. Experimental Setup

Table 1 provides an overview of the event logs used in our experimentation. *Sepsis* has a relatively high number of different trace variants, all of which have comparable frequencies, with the most frequent trace making up only 3.33 % of the event log. Activities are repeated often within a trace, which must lead to looping behavior within a Petri net with uniquely labeled transitions. *RTFM* is rather large, with a moderate variety of trace variants and activities. Both for variants and activities some are very frequent while others are quite infrequent. *Teleclaims* is an established artificial log useful for testing discovery of various control-flow structures. With *Orders* we can demonstrate the algorithm's ability to discover complex control flow structures, as well as the option to abstract from rare behavior. For each event log we perform 8400 runs of the algorithm with varying combinations of the different parameters, as specified in Table 2. Note that we keep the order of place candidate traversal fixed for all runs.

Our experiments with combined fitness have shown that only for the *Sepsis* log there are place candidates that score lower on relative fitness than aggregate fitness. However, this happened for very few parameter combinations and then only for at most 2 candidate places. Thus, we can conclude that the choice between using fm_{agg} and fm_{comb} does not have a significant impact for the logs evaluated.

Table 1. List of logs used for the evaluation. The upper part lists real-life logs while the lower part shows artificial logs. Logs are referred to by their abbreviations.

Log Name	Abbreviation	Activities	Trace Variants	Reference
Sepsis	Sepsis	16	846	[30]
Road Traffic Fine Management	RTFM	11	231	[31]
Teleclaims	Teleclaims	11	12	[28]
Order-Handling	Orders	8	9	[32]

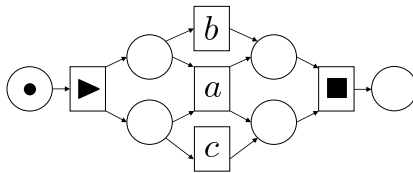


Figure 16. An example model used to illustrate the applied quality metrics.

Evaluation Metrics

Our goal is the discovery of a model which can express the behavior in the event log (fitness), does not allow for much additional behavior not seen in the event log (precision), and is not unnecessarily complex (simplicity). Furthermore, since we assume the user can filter the event log with respect to uninteresting events and trace variants and is therefore interested also in the control-flow of infrequent activities, we evaluate models with respect to how many activities from the event log have a corresponding transition in the Petri net (activity-coverage). Several approaches exist to measure model quality with respect to an event log. In the following, we give a brief overview of the techniques applied in the context of this evaluation.

The eST-Miner evaluates places locally, and does not aim to simply maximize the number of perfectly replayable traces but rather to discover patterns with high support over the whole event log, as illustrated by the motivational example in Figure 1. Therefore, we use alignments to compute fitness to measure how well the behavior in the log is represented by the model. Alignments take an event log and compute the minimal number of insertions and deletions needed to make the traces fitting with respect to a given model, then normalize this value using the worst-case edit distance. Consider the example Petri net in Figure 16 and the trace $\langle \blacktriangleright, a, b, c, \blacksquare \rangle$. This trace can be aligned to the Petri net by, for example, removing b and c or by removing a . Removing a needs 1 edit operation, which is the optimum in this case. The worst-case edit distance would require us to remove every activity from the trace (5) and insert an activity for every transition that needs to be fired to obtain the shortest path through the model (3). This results in an alignment-based fitness of $1 - \frac{1}{5+3}$ for the example trace. For details, we refer the reader to ([33]).

Evaluating whether the model is sufficiently restrictive, i.e., does not allow for (much) behavior outside of the process behavior is more challenging. The event log represents a set of example process executions and cannot be expected to be complete, making it hard to reliably evaluate process-

Table 2. Overview of the parameters settings used in our experimentation. The combinations result in 8400 runs for each event log. The value ranges were chosen based on a smaller set of preliminary experiments, aiming to investigate a wide range of parameter settings on the one hand, while on the other hand avoiding unnecessary complexity resulting from variation without notable impact. For example, for our inputs no places were discarded for $|Q| \geq 10000$. For d^+ we chose a very low and a very high value to evaluate whether it had any impact at all. Finally, for the chosen event logs $d_{cut} = 5$ has shown to be sufficient to find complex structures with the standard eST-Miner, i.e., increasing the traversed tree depth increases computation time but has no strong impact on model quality.

Parameter	Used Values	Purpose
τ	0.3, 0.4, 0.5, 0.6, 0.7, 0.8, 0.9	Defines the minimal fraction of log traces that every place, as well as the final Petri net, must be able to replay.
δ	0.05, 0.1, 0.15, 0.2, 0.25	Used to define the allowed reduction in log traces replayable by N when adding a place.
fm	fm_{rel} , fm_{comb}	Defines the fitness metric to be used.
adapt	$adapt_{noDelta}$, $adapt_{constant}$, $adapt_{linear}$, $adapt_{sigmoid}$	The delta adaption function used to guide the heuristics.
s	1, 2, 3, 4, 5	The steepness of the increase of the adaption function (relevant for $adapt_{linear}$ and $adapt_{sigmoid}$ only).
$ Q $	100, 1000, 10000	The maximal number of places stored in Q .
d^+	0, 10	Artificial tree depth to re-evaluate places in Q after end of tree traversal (relevant for $adapt_{linear}$ and $adapt_{sigmoid}$ only).
d_{cut}	5	Stop candidate traversal after the specified tree level.

related precision. Another problem is the potentially infinite language of the model which can make a straightforward comparison infeasible. Therefore, metrics that approximate precision are commonly used. We choose a precision metric based on escaping edges. This metric compares the number of activities enabled in the model with the number of activities actually executed during the replay of the event log. Consider the example Petri net in Figure 16 and the traces $\langle \blacktriangleright, a, \blacksquare \rangle$ and $\langle \blacktriangleright, c, b, \blacksquare \rangle$. We replay all prefixes of traces in the event log and take note of the frequency of that prefix, the number of enabled transitions at the end of the prefix and the number of transitions fired after the prefix. In our example, for both traces in the beginning only \blacktriangleright is enabled and consequently fired ($2 \cdot 1$ enabled, $2 \cdot 1$ fired). This enables three activities a, b and c , of which we fire a in the first trace and c in the second trace ($2 \cdot 3$ enabled, $2 \cdot 2$ executed). Now, for the first trace \blacksquare is the only one executed and fired ($1 \cdot 1$ enabled, $1 \cdot 1$ fired). For the second trace, after firing c only b is enabled and fired ($1 \cdot 1$ enabled, $1 \cdot 1$ fired) followed by the final activity, \blacksquare , being enabled and fired ($1 \cdot 1$ enabled, $1 \cdot 1$ fired). This results in a precision of $\frac{2 \cdot 1 + 2 \cdot 2 + 1 \cdot 1 + 1 \cdot 1 + 1 \cdot 1}{2 \cdot 1 + 2 \cdot 3 + 1 \cdot 1 + 1 \cdot 1 + 1 \cdot 1} = \frac{9}{11}$, i.e., the number of transitions actually fired during

replay divided by the number of enabled transitions. For details on escaping edges precision we refer the reader to ([34]).

We want to avoid the removal of infrequent activities and thus aim for a Petri net that ideally includes one transition for each activity in the event log, i.e., the lower the number of dead transitions removed by our approach, the better. We introduce the metric of *activity-coverage* to reflect this.

Definition 8.1. (Activity-Coverage)

Let L be an event log over the set of activities A and let $N = (A', P)$ be a Petri net with $A' \subseteq A$, i.e., A' is the subset of log activities included in the Petri net N . We define *activity-coverage* of N with respect to L as

$$\text{activity-coverage}_L(N) = \frac{|A'|}{|A|}$$

The simplicity of a model is highly subjective and a variety of factors may contribute to the readability of a model. Not all of these can be easily represented by numbers, e.g., the way a Petri net is plotted. Therefore, we forgo an extensive evaluation of simplicity and focus on a straightforward metric to express the fraction of net elements that are transitions, arguing that a Petri net with relatively few places is likely to be perceived as simple.

Definition 8.2. (Simplicity)

Given a Petri net $N = (A, P)$, we define *simplicity* as the fraction of nodes that are transitions, i.e.,

$$\text{simplicity}(N) = 1 - \frac{|P|}{|P| + |A|}.$$

The example Petri net in Figure 16 achieves a simplicity of $1 - \frac{6}{6+5} = \frac{5}{11}$.

A value of 1 indicates that all activities in the event log are also part of the Petri net, while a value of 0 indicates that no activity in the event log is part of the Petri net. With respect to the event log $L = [\langle \blacktriangleright, a, \blacksquare \rangle, \langle \blacktriangleright, c, b, \blacksquare \rangle, \langle \blacktriangleright, d, e, d, e, a, \blacksquare \rangle]$, the example Petri net in Figure 16 achieves an activity-coverage of $\frac{3}{5}$.

All used quality metrics return values between 0 and 1, where a value close to 1 indicates high quality in general. However, note that for simplicity, a value around 0.5 indicates a model with roughly as many places as transitions, for example, a simple sequence, while a higher value would arise from a Petri net with extremely few places. Therefore, we consider a value close to 0.5 to be close to optimal in terms of simplicity.

One can assign a general quality score to a model that summarizes the scores achieved in the different quality aspects. One commonly used metric in the context of process mining is the F_1 -score, the harmonic mean of fitness and precision. This ensures that the resulting aggregated quality score reflects both metrics, i.e., a low value in one of the metrics cannot be obscured by a high value in the other.

Definition 8.3. (F_1 -Score)

Given an event log L and a Petri net N with a fitness score of $\text{fitness}_L(N)$ and a precision score of $\text{precision}_L(N)$, we define the F_1 -score as

$$F_1(L, N) = \frac{2}{\frac{1}{\text{fitness}_L(N)} + \frac{1}{\text{precision}_L(N)}}$$

Since we are interested in models that represent behavior of infrequent activities as well, we define an alternative aggregated quality score which includes activity-coverage.

Definition 8.4. (HM-Score)

Given an event log L and a Petri net N with a fitness score of $\text{fitness}_L(N)$ and a precision score of $\text{precision}_L(N)$, we define the HM-score as

$$\text{HM}(L, N) = \frac{3}{\frac{1}{\text{fitness}_L(N)} + \frac{1}{\text{precision}_L(N)} + \frac{1}{\text{activity-coverage}_L(N)}}$$

8.2. Qualitative Analysis

Some interdependencies between the model quality aspects are to be expected and confirmed by our results. Removing a transition from a Petri net reduces the behavior of the net and therefore has a negative effect on fitness and a positive effect on precision. It is important to keep in mind the exact metrics used to measure fitness and precision to avoid misinterpretation of the results: while alignments are quite forgiving with respect to missing infrequent transitions (they simply assign a penalty whenever the corresponding activity occurs in the event log), escaping edges based precision is sensitive with respect to transitions that are frequently enabled without being fired (e.g. in the case of parallelism).

One of our major goals in this work is to avoid the removal of transitions based on infrequency. By achieving this goal, we obtain models that contain transitions which are far more often enabled than fired. Such models score significantly worse with respect to precision than models without those infrequent transitions, while fitness remains comparable. In an attempt to balance these effects, we do not only use the harmonic mean of fitness and precision (F_1) to approximate model quality as is commonly done, but additionally define a summarizing score that also includes activity-coverage (HM). Additionally, we focus on models with perfect activity-coverage by evaluating them separately from the complete set of results. Finally, we include some representative models to support the interpretation of the number-based evaluation. However, the choice of the best model always depends on the user's needs and models scoring high in the context of this general evaluation do not necessarily represent the best model for every application.

Overview of Quality Results

In Figure 17, an overview of the quality results of the 8200 models generated for each log is given. Fitness and simplicity remain rather stable, with fitness being generally high and simplicity values clustering around 0.5 (which we consider a good value, recall Definition 8.2). On the other hand, precision and activity-coverage, and by extension the harmonic means HM and F_1 , vary a lot for the discovered models. This clearly indicates that the choice of parameters has a strong impact on these quality aspects.

While we discovered only 7 unique models for *Orders*, there were 35 unique models found for *RTFM*, 43 for *Teleclaims* and 191 for *Sepsis*. The quality results and frequencies of a selected subset of the discovered Petri nets are given in Table 3. Additionally, we provide the same results for

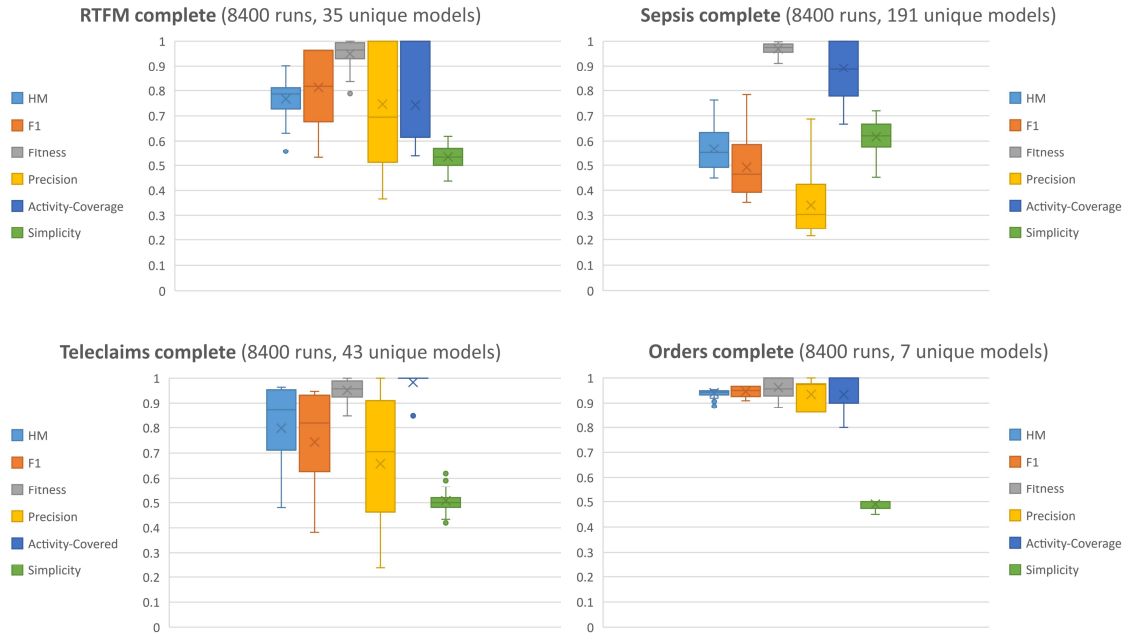


Figure 17. Overview of model quality results for all 8400 runs (complete) with varying parameters but fixed candidate traversal order.

Table 3. Overview of the qualitative results of selected models discovered during our experimentation. For each log we show the quality results of the model with the maximal HM value, the maximal F_1 value, and the model with the maximal HM out of the subset of models with perfect activity-coverage (aCov), as well as the frequency with which this model was discovered. Additionally, we provide scores for the Inductive Miner infrequent (IMf, default settings) and the eST-Miner with $\tau = 1.0$. Green background marks comparatively large values. All of these models are also visualized in Figures 20 to 23 at the end of the section.

Metric	RTFM					Sepsis					Teleclaims					Orders				
	For Comparison		Selection of Discovered Models			For Comparison		Selection of Discovered Models			For Comparison		Selection of Discovered Models			For Comparison		Selection of Discovered Models		
	IMf (default)	eST ($\tau=1.0$)	Max. HM	Max. F1	HM (aCov)	IMf (default)	eST ($\tau=1.0$)	Max. HM	Max. F1	HM (aCov)	IMf (default)	eST ($\tau=1.0$)	Max. HM	Max. F1	HM (aCov)	IMf (default)	eST ($\tau=1.0$)	Max. HM	Max. F1	HM (aCov)
HM	0.7300	0.7385	0.9018	0.8108	0.9018	0.4154	0.4212	0.7620	0.7620	0.5854	0.9659	0.6917	0.9640	0.9640	0.9640	0.9550	0.9536	0.9536	0.9432	0.9536
F1	0.6432	0.6531	0.8596	0.9638	0.8596	0.3215	0.3266	0.7836	0.7836	0.4849	0.9496	0.5993	0.9469	0.9469	0.9469	0.9340	0.9319	0.9319	0.9664	0.9319
Fitness	0.9820	1.0000	0.8747	0.9301	0.8747	0.9060	1.0000	0.9115	0.9115	0.9679	0.9490	1.0000	0.9244	0.9244	0.9244	0.9600	1.0000	1.0000	0.9562	1.0000
Precision	0.4782	0.4849	0.8451	1.0000	0.8451	0.1954	0.1952	0.6871	0.6871	0.3235	0.9503	0.4279	0.9706	0.9706	0.9706	0.9094	0.8725	0.8725	0.9768	0.8725
Activity-Coverage	1.0000	1.0000	1.0000	0.6154	1.0000	1.0000	1.0000	0.7222	0.7222	1.0000	1.0000	1.0000	1.0000	1.0000	1.0000	1.0000	1.0000	1.0000	0.9000	1.0000
Simplicity	0.5526	0.6842	0.5200	0.5000	0.5200	0.7826	0.7826	0.5200	0.5200	0.5806	0.5172	0.5200	0.5200	0.5200	0.5200	0.5000	0.4762	0.4762	0.4737	0.4762
Frequency	-	-	150	2276	150	-	-	90	90	180	-	-	300	300	300	-	-	64	2852	64

the models discovered by the Inductive Miner infrequent (IMf) with default settings as implemented in ProM [27] and the models discovered by the eST-Miner with $\tau = 1.0$ (comparable to region theory results). Our approach can discover models with HM and F_1 scores that clearly outperform IMf with default settings as well as eST with $\tau = 1.0$ on the two real-life event logs. For the two artificial event logs results are comparable. A detailed comparison of these models follows at the end of this section.

Discussion of Dead Transitions

Since we are interested in abstracting from infrequent behavioral patterns without outright removal of infrequent activities or complete trace variants, we take a closer look at the discovery of models that include all activities from the event log. During our experimentation, we discovered 2 different such models for *Orders*, 40 for *Teleclaims*, 33 for *Sepsis* and 9 for *RTFM*.

In Figure 18, we show an overview of the quality metrics restricted to the multiset of discovered models that include all activities. The general tendencies remain similar to the results shown for the models discovered for the complete set of runs. Fitness is consistently high, with less lower scoring outliers than we have seen for the complete set of models. This is to be expected, since these models do contain all log activities and our proposed approach guarantees that they can all be fired at least once. Consequently, precision is comparable for the artificial logs which do not include a lot of noise or diverse behavior, or lower for the real-life logs, which exhibit a significantly higher variance in behavior. Notably, the number of models and variance in precision have decreased for *Sepsis* and *Orders* - apparently, the parameter combinations allowing for the discovery of models without dead transitions do result in models scoring similarly in quality.

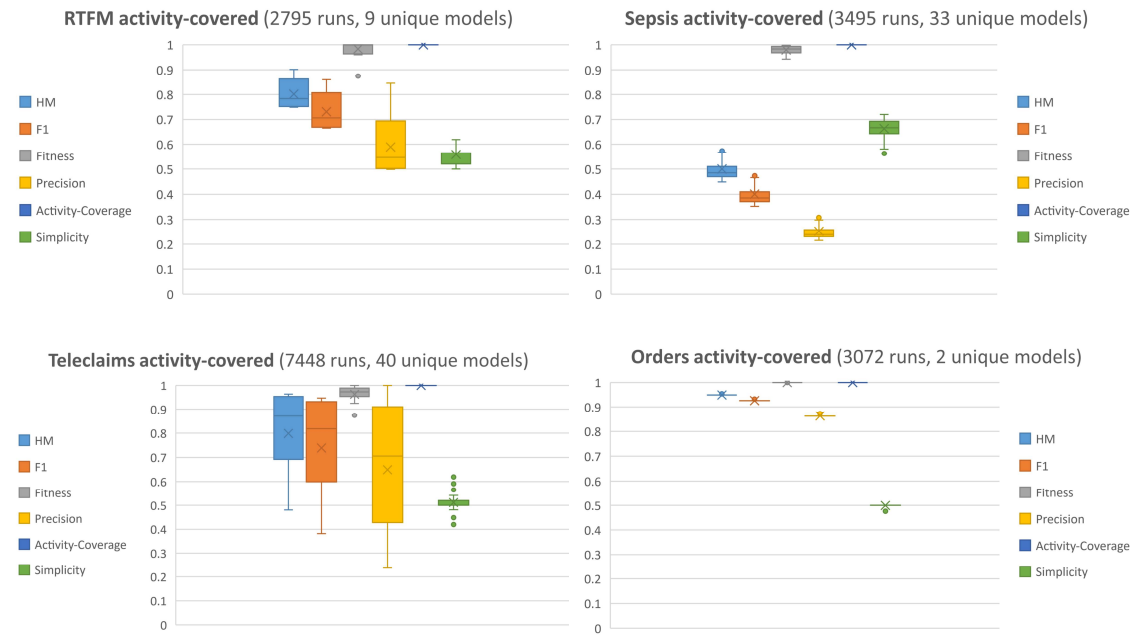


Figure 18. Overview of quality results for all models discovered in the 8400 runs that include all activities observed in the corresponding event log.

In Section 5, we introduced *combined fitness* with the goal of preventing the uncontrolled deletion of infrequent activities due to their execution being blocked accidentally. In Figure 19, we compare the impact of using combined fitness and of using relative fitness on the number of dead transitions in the discovered models. In particular for the two real-life event logs, *Sepsis* and *RTFM*, a clear effect is visible: when using combined fitness is it much more likely to discover models which include

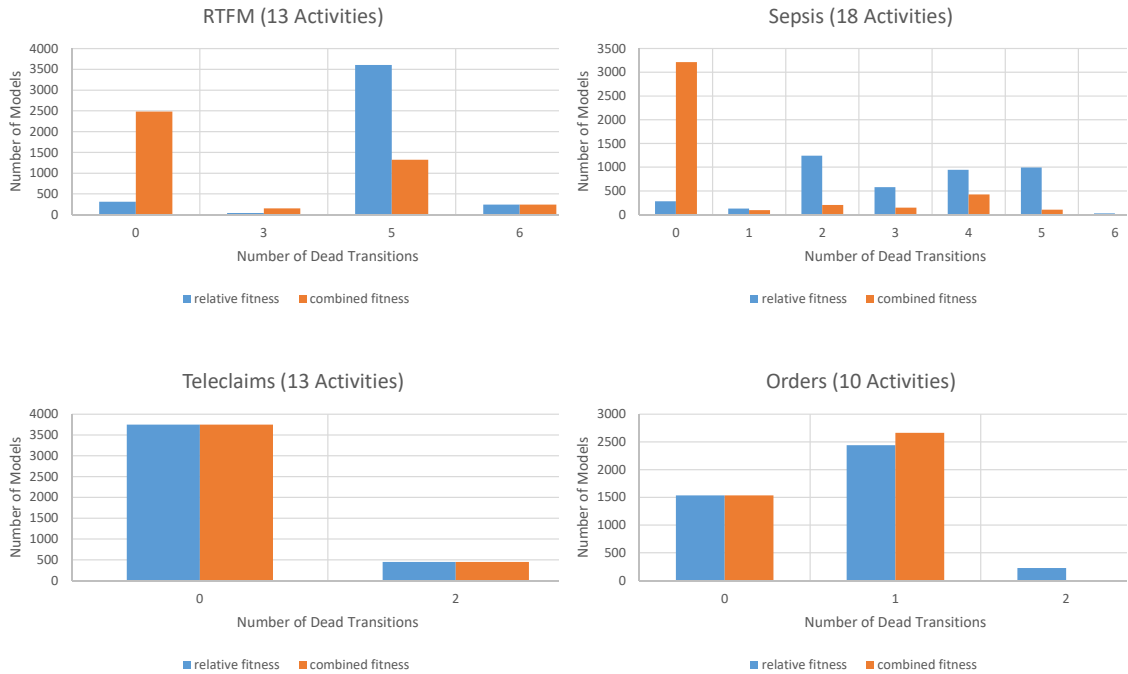


Figure 19. Comparison of the number of dead transitions of the models discovered using *relative fitness* and using *combined fitness* with the proposed algorithm.

all or most of the observed activities. This observation confirmed by the data in Table 4 where we compare the number of runs that result in models without dead transitions for the runs using combined fitness and the runs using relative fitness. Teleclaims is the only exception to this rule - for this artificial event log the majority of parameter combinations result in models without dead transitions, independently of the fitness metric chosen. Similar tendencies can be observed for the number of different models without dead transitions; especially for the two real-life logs, most such models are discovered using combined fitness.

Another interesting aspect can be observed for the RTFM and Teleclaims event logs: models with certain numbers of dead transitions (1, 2, 4 for RTFM, 1 for Teleclaims) are never discovered. This can be explained by groups of transitions which are closely coupled in behavior and (almost) always occur together in the same traces. They are removed from the model together once these traces are no longer replayable. Examples are the activities *S check if sufficient information is available* and *S register claim* in the Teleclaims log or *Insert Date Appeal to Prefecture* and *Send Appeal to Prefecture* in the RTFM log.

Table 4. Out of the 8400 runs we performed in our experiments, 4200 were performed using *combined fitness* and 4200 using *relative fitness*. For each event log this table gives an overview about the number of runs that resulted in models without dead transition, as well as how many different such models were discovered.

	combined fitness (4200 runs)		relative fitness (4200 runs)	
	#runs	#unique models	#runs	#unique models
RTFM	2483	8	312	1
Sepsis	3143	30	352	4
Teleclaims	3698	23	3750	24
Orders	3004	1	64	2

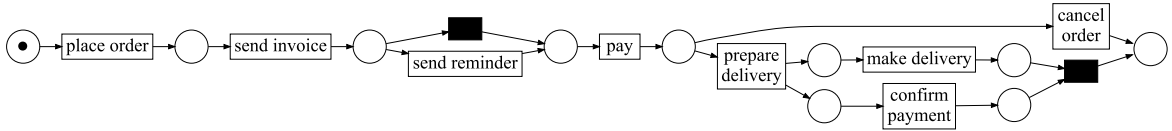
Discussion of Selected Models

In Figures 20, 21, 22 and 23 we present a selection of models for each log. For comparison, we present the models discovered by IMf (default settings) and the model discovered by the eST-Miner with $\tau = 1.0$. From the many models discovered during the experimentation with our approach, we show the models scoring highest with respect to HM (the harmonic mean of fitness, precision, activity-coverage) as well as with respect to F_1 (harmonic mean of fitness and precision only). Furthermore, we present the models with the highest HM and F_1 values out of the set of models without dead transitions. Of course, while these models score highest with respect to the general quality metrics used in this evaluation, other models may still be considered to be more suitable for specific contexts or applications.

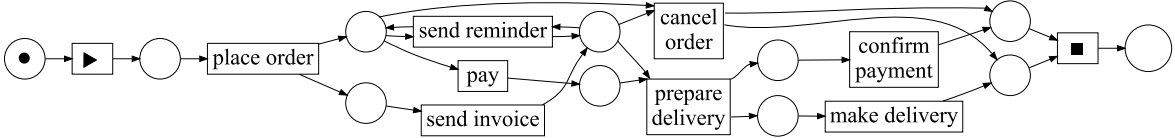
All models shown in Figure 20 were discovered for the Orders log. For this rather simple event log, all models achieve relatively high scores with respect to the quality metrics. However, some notable differences in the expressed behavior can be observed in particular with respect to the activities *send invoice*, *send reminder*, *pay* and *cancel order*. According to the event log, in most cases the execution of *send invoice* is eventually followed either by *pay* (and then delivery) or by *cancel order*, but never both. In rare cases, payment occurs before sending the invoice. After sending the invoice, reminders can be sent repeatedly, until payment is received or the order is canceled. This behavior is fully expressed only by the model discovered using the eST-Miner with $\tau = 1.0$, which is comparable to results produced by region-based approaches. Since payment before sending the invoice is rare, users may prefer the other models which focus on behavior where payment arrives after sending the invoice. The model discovered by IMf further deviates from the log by not allowing for repeated reminders (occurring in 25 % of the traces), and enabling the cancellation of orders after payment. The model with the highest HM value is the same for both, the complete set of models as well as the set without dead transitions. It includes all activities observed in the event log, in contrast to the model with the highest F_1 -Score, which does not contain the activity *cancel order* (occurring in 13.03 % of traces) at all, resulting in slightly lower fitness but increased precision.

The Sepsis event log exhibits many repetitions of activities and a comparatively high control-flow variance, with 846 trace variants in 1050 traces, the most frequent of which occurs only 35 times. Thus, the discovery of a model with simultaneously high fitness and precision is challenging. Figure 21 presents a selection of discovered Petri nets. The IMf manages to discover groups of activities

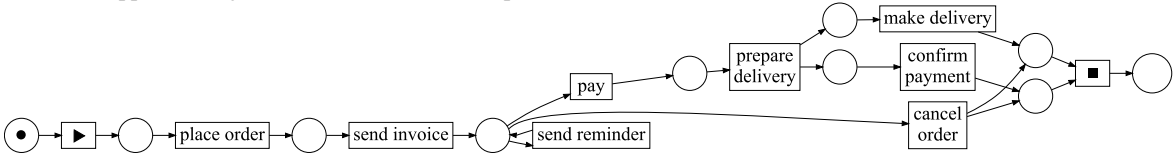
Inductive Miner infrequent (default settings):



eST-Miner ($\tau = 1.0$):



Presented Approach: highest HM value out of the complete set of results, as well as the set of models without dead transitions.



Presented Approach: highest F_1 -score out of the complete set of results.

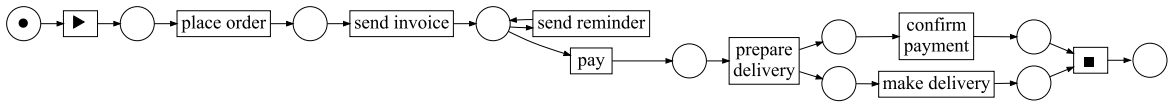
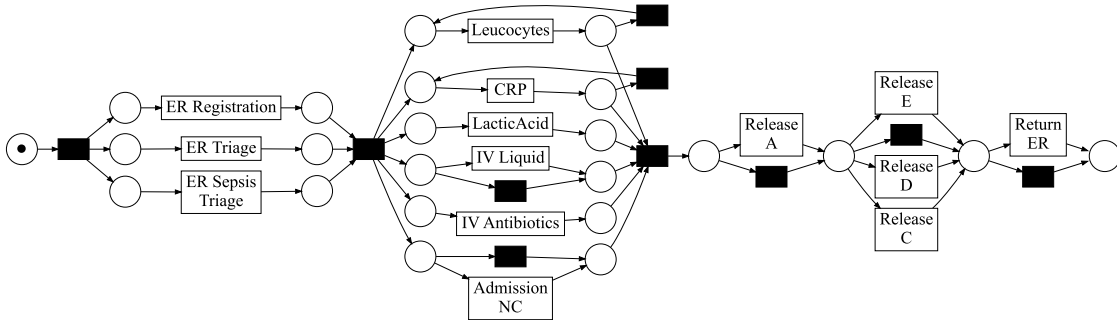


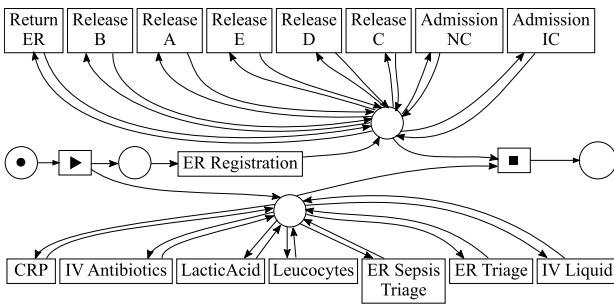
Figure 20. The Petri nets discovered based on the `Orders` log using the Inductive Miner infrequent (default settings), the eST-Miner with $\tau = 1.0$, and a subset of interesting models discovered using the presented approach.

that occur in sequence, however, within these groups the activities are in parallel and mostly skippable, resulting in a very low precision. The eST-Miner with $\tau = 1.0$ illustrates a disadvantage of requiring perfect fitness: the resulting model allows for nearly all possible behaviors. For the model with highest HM value out of all models without dead transitions, this problem becomes less severe. Finally, the model with highest HM and F_1 values out of all discovered models manages to capture the main behavior hidden in the traces while ignoring infrequent activity behavior, achieving comparatively high precision at the cost of not representing all activities.

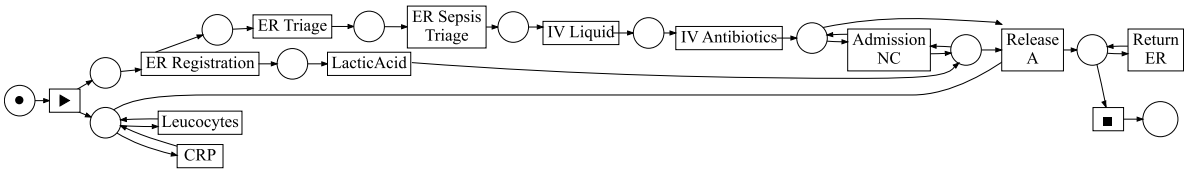
Inductive Miner infrequent (default settings):



eST-Miner ($\tau = 1.0$):



Presented Approach: highest HM value and highest F_1 -score out of the complete set of results.



Presented Approach: highest HM value out of the set of models without dead transitions.

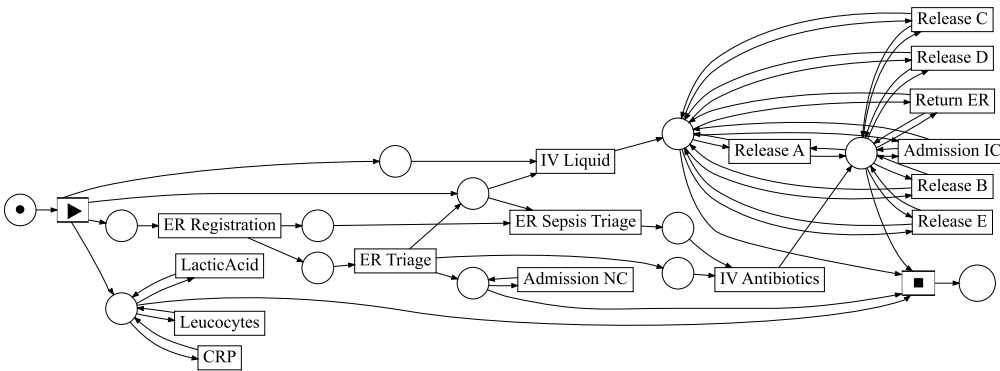
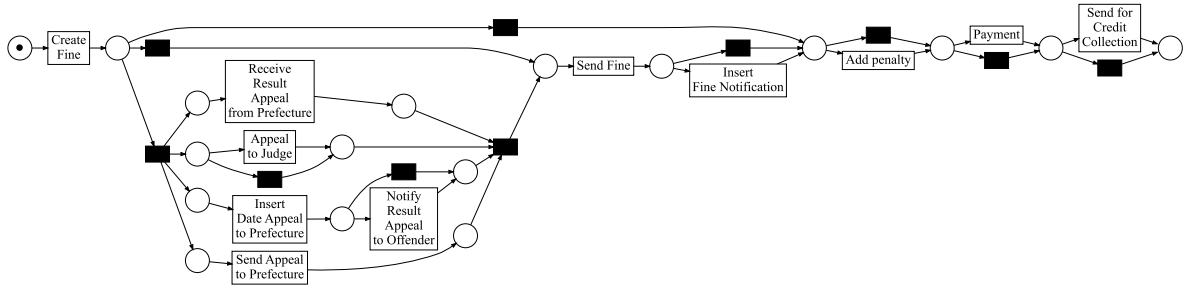
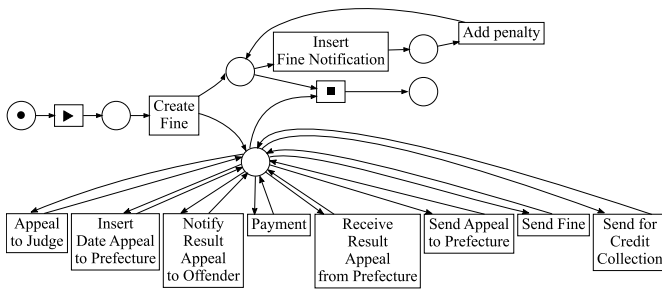


Figure 21. The Petri nets discovered based on the Sepsis log using the Inductive Miner infrequent (default settings), the eST-Miner with $\tau = 1.0$, and a subset of interesting models discovered using the presented approach.

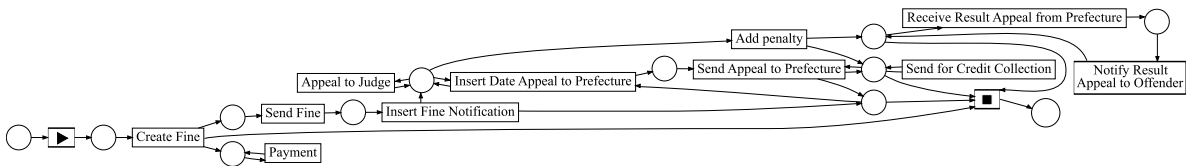
Inductive Miner infrequent (default settings):



eST-Miner ($\tau = 1.0$):



Presented Approach: highest HM value out of the complete set of results, as well as the set of models without dead transitions.



Presented Approach: highest F_1 -score out of the complete set of results.

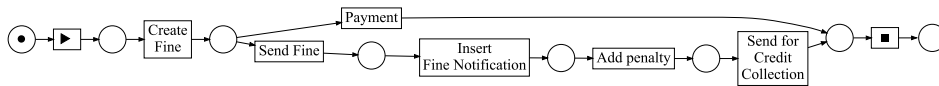
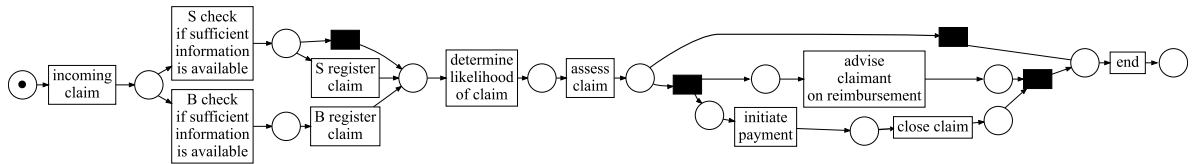


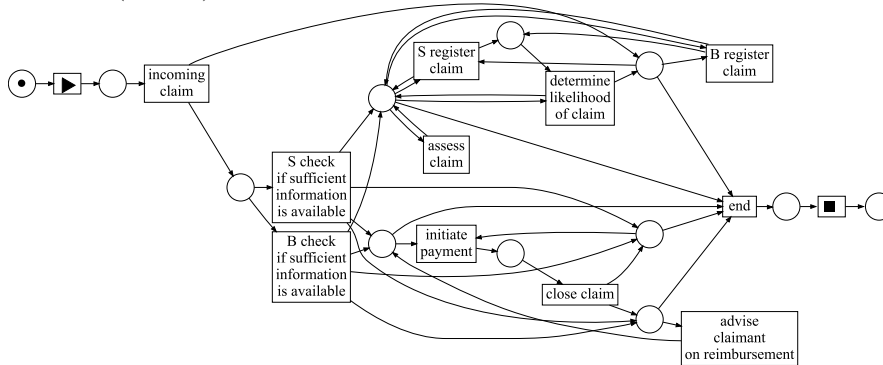
Figure 22. The Petri nets discovered based on the RTFM log using the Inductive Miner infrequent (default settings), the eST-Miner with $\tau = 1.0$, and a subset of interesting models discovered using the presented approach.

Figure 22 shows Petri nets discovered from the RTFM log. Considering the models discovered by IMf and eST-Miner with $\tau = 1.0$, we observe the same general tendencies as for the previous logs. For the model with the highest F_1 -score discovered by our approach, we note that several activities are missing, meaning that they are not part of any replayable trace from the event log. The reason can be found by investigation of this particular event log, which describes two very distinct sub-processes, the more frequent of which consists of the activities still contained in the model. The activities of the infrequent sub-process related to appeals have been removed, allowing to focus on the main process. The model with the highest HM includes all activities from the event log. It includes the main process which is also expressed by the model with highest F_1 , with additional self-loops that model optionality of those activities. Additionally, the control-flow of the appeal-related subprocess is included. Here, self-loops are not only used to model skippable activities but also to enforce a certain order on the events. Despite the limitations of using only uniquely labeled transitions, the positioning of the infrequent activities within the control-flow is precise and reflects their behavioral patterns in the event log.

Inductive Miner infrequent (default settings):



eST-Miner ($\tau = 1.0$):



Presented Approach: highest HM value and highest F_1 -score out of the complete set of results, as well as the set of models without dead transitions.

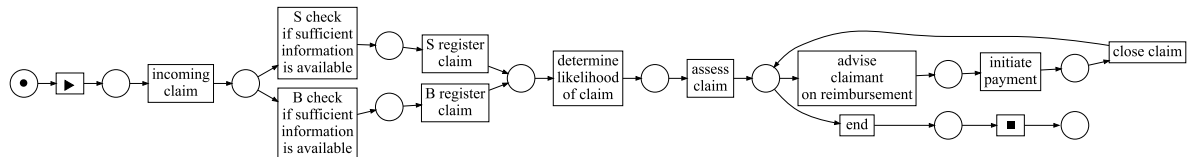


Figure 23. The Petri nets discovered based on the Teleclaims log using the Inductive Miner infrequent (default settings), the eST-Miner with $\tau = 1.0$, and a subset of interesting models discovered using the presented approach.

A set of process models discovered from the Teleclaims log is presented in Figure 23. For this event log, the same model scores highest with respect to HM and F_1 for the complete set of discovered models as well as for the set of models without dead transitions. This model and the model discovered by IMf express similar behavior, with the main difference being the representation of skippable activities: with all transitions being uniquely labeled, our approach has to rely on loop constructs rather than silent activities. The eST-Miner with $\tau = 1.0$ does not abstract from infrequent behavior, which in this case results in a perfectly fitting but quite complex model.

Our results confirm the expectation that even minor gains in fitness are usually accompanied by a major drop in precision. The models with the best F_1 -Score are usually those with the highest precision value. From Figures 20 to 23 we can observe that these models seem to abstract well from rarely occurring behaviors, giving a clear representation of the control-flow of the main activities. However, they may not incorporate behavior of infrequent process variations, even if they do follow a well-defined execution path. This is clearly illustrated by the Orders and RTFM event logs. Here, infrequent but potentially vital paths in the control-flow (e.g. cancellation of an order or appeal against a fine) can be revealed when the discovery algorithm abstracts from chaotic behavioral patterns without ignoring infrequent activities themselves. The presented approach is able to return models anywhere on the scale balancing fitness, precision and activity-coverage, based on the choice of parameters.

Impact of Parameter Choices

While the quality results discussed earlier clearly indicate that our approach is able to discover models balancing fitness, precision and activity-coverage while maintaining reasonable simplicity, the choice of parameters has a significant impact. Therefore, we investigate this further. We used decision tree analysis to search for parameter settings that would result in the highest quality models as indicated by the HM-Score. Since, for some event logs, the best model according to this metric was discovered very infrequently, we extended the notion to the top 5% of runs. However, in other logs the best model was discovered in significantly more than 5% of the runs. This discrepancy resulted in an imbalance of the absolute number of runs resulting in the highest-scoring model(s). Additionally, we performed the same analysis approach for the set of models without dead activities, again looking for the (at least) 5% of runs which resulted in models with the highest HM value.

The results of this analysis are shown in Figure 24, where each line represents a set of parameter combinations that leads to the discovery of the best model(s). Information on the frequency and entropy of the corresponding leaf in the decision tree is included as well.

	Best 5% of	Leaf Entropy	Frequency	\mathcal{T}	Adaption Strategy	δ	fm	s	d*
Sepsis	complete (637)	0	300	0.3	adapt _{noDelta}				
		0.014	144		adapt _{constant} adapt _{linear} adapt _{sigmoid}	0.25		[2,5]	
		0	60		adapt _{constant}	[0.15,0.2]	fm _{rel}		
		0.153	36		adapt _{linear}			[3.5]	
	perfect activity coverage (216)	0	150	0.7	adapt _{noDelta}		fm _{rel}		
RTFM	complete (510)	0	150	0.5	adapt _{noDelta}		fm _{comb}		
		0	150	0.8	adapt _{noDelta}				
		0	135		adapt _{constant} adapt _{linear} adapt _{sigmoid}	[0.15, 0.25]			10
		0	30		adapt _{linear}	[0.05,0.1]			
		0	45		adapt _{constant}	[0.15,0.25]			0
	perfect activity coverage (150)	0	150		0.5	adapt _{noDelta}		fm _{comb}	
Teleclaims	complete (716)	0	360	[0.3,0.4]	adapt _{constant}	[0.15,0.25]			
		0.219	192		adapt _{linear} adapt _{sigmoid}	[0.2,0.25]		[4,5]	
		0	48		adapt _{linear}	0.15		[3,4]	
	perfect activity coverage (716)	0	360	[0.3,0.4]	adapt _{constant}	[0.15,0.25]			
		0.219	192		adapt _{linear} adapt _{sigmoid}	[0.2,0.25]		[4,5]	
		0	48		adapt _{linear}	0.15		[3,4]	
Orders	complete (3072)	0	1200	0.9					
		0	1440	[0.3,0.8]	adapt _{constant} adapt _{sigmoid}	[0.05,0.1]			
		0	180		adapt _{linear}	0.05			
		0	108		adapt _{linear}	[0.15, 0.25]	1	0	
		0.444	72		adapt _{sigmoid}				
	perfect activity coverage (3072)	0	1200		0.9				
		0	1440	[0.3,0.8]	adapt _{constant} adapt _{sigmoid}	[0.05,0.1]			
		0	180		adapt _{linear}	0.05			
		0	108		adapt _{linear}	[0.15, 0.25]	1	0	
0.444		72	adapt _{sigmoid}						

Figure 24. Overview of the parameter choices resulting in the discovery of the models with the top 0.05 fraction of the HM value, once for all discovered models and once for the models with perfect activity-coverage. For each log, we indicate how often such models have been discovered in our experimentation. Each line presents to a set of parameter combinations, with the frequency and entropy of the corresponding leaf node in the decision tree. For each parameter that our decision tree analysis has revealed to be impactful, the possible values are indicated. Empty cells indicate that the corresponding parameter was insignificant for reaching the leaf. Leaves which did not include a significant number of positive instances have are not included, resulting in a slight discrepancy between the number of such models discovered and the sum of leaf frequencies.

For *Sepsis* the overall best scoring model requires the lowest investigated value of τ , that is 0.3. Additionally, δ should either be ignored completely by using the $\text{adapt}_{noDelta}$ adaption function or set to the largest value. Slightly lower values of δ paired with the less constraining relative fitness can be combined with $\text{adapt}_{constant}$, i.e., always using the maximum value for δ , or adapt_{linear} with larger steepness values. All in all, the parameters indicate that rather restricting places with comparatively low fitness must be accepted to discover models with higher quality for the *Sepsis* log. This makes sense in the context of the large variety of traces without clear main behavior, i.e., all trace variants have similarly low frequency. However, the large HM value of the models discovered with those parameter settings is mostly based on scoring high precision, which is also due to 5 activities not being included. Choosing $\tau = 0.7$ together with relative fitness and no δ -based limitation ($\text{adapt}_{noDelta}$) balances fitness and precision such that the highest-scoring model that includes all log activities can be discovered.

For the *RTFM* event log the use of combined fitness is a prerequisite to discovering the best-scoring models. In contrast to *Sepsis*, larger values of τ seem important: a choice $\tau = 0.5$ or $\tau = 0.8$ while ignoring δ ($\text{adapt}_{noDelta}$) results in a high-quality model. In particular, $\tau = 0.5$ results in the highest scoring model without dead transitions. Alternatively, $\tau = 0.8$ can be combined with large values of δ and/or lenient delta adaptations, e.g., adaptations functions combined with a larger steepness value to quickly grow more permissive, or with artificial tree depth.

For the *Teleclaims* event log the set of best-scoring models coincides with the set of best-scoring models without dead transitions. A τ value of at most 0.4 is a prerequisite. Combining a $\delta \geq 0.15$ with the constant adaption function results in a high-quality model. Gradually adapting δ using linear or sigmoid adaption requires larger values of δ and high steepness s . The linear adaption, which grows the adapted δ faster in the beginning, allows for these values to be slightly lower.

The set of best-scoring models in general and best-scoring models with perfect activity-coverage is the same for the *Orders* event log. To discover such models, one can simply pick the highest τ value of 0.9. Alternatively, restrictiveness can be shifted from τ to δ by combining lower values of τ with lower values of $\delta \leq 0.1$ and another adaption function than $\text{adapt}_{noDelta}$.

For the four event logs investigated in this paper, the most important parameter seems to be τ . This is not surprising, since τ has a direct impact on which places are available for addition to the Petri net. In some cases, e.g. the *Orders* event log, it seems possible to compensate a low value of τ (permissive) with a low adapted value of δ (restrictive). Most other parameters appear in combination with certain choices for δ , which makes sense since on the one hand δ is limiting the range of the adaption strategies, which include the use of s , and on the other hand a low value of δ can be ignored using $\text{adapt}_{noDelta}$.

Notably, the artificial tree depth d^+ as well as $|Q|$ have had no major impact on the discovery of any of the examined models. The length of the potential places queue $|Q|$ never showed up as a decisive factor at all and d^+ appeared rarely and always alternatives using other parameters to obtain the same models existed. Furthermore, the sigmoid and linear delta adaption strategies seem mostly interchangeable, even though the linear function seems to be preferred in combination with slightly lower values of δ . The reason may be that it allows for a faster initial growth of the adapted δ .

Surprisingly, the choice of the fitness metric seems less important for discovering the best model than the previous results have indicated. One may have expected that combined fitness would turn

out to be critical in particular when searching for models without dead transitions. This expectation was confirmed only for the RTFM event log. However, combined fitness is more restrictive, making higher precision harder to achieve. Thus, while the use of relative fitness results in models including all observed activities significantly less frequent than when using combined fitness, if such a model is discovered its precision score is likely to be higher.

Some interdependencies between the parameters are expected, and seem to be confirmed by the results in Figure 24. For event logs like the RTFM log and the Orders log, which have a few very dominant trace variants, we seem to generally achieve good results for rather high values of τ or very restrictive δ . In contrast, for event logs with a high variety of traces, as for example Sepsis log, a low τ -value seems mandatory. Most likely, the large variety of fitting places allows for obtaining high precision, while our heuristics seems to successfully ensure the focus on the main behavioral patterns.

Indeed, the results from the Sepsis log, which contains a high variety of traces, seem to confirm our algorithms ability to discover the main behavior hidden in an event log even in the absence of main trace variants: for a low value of τ , e.g. $\tau = 0.3$, the fraction of log traces replayable by the return Petri net is indeed close to 0.3, however, the alignment-based fitness reliably remains above 0.9, indicating that most of the traces are close to being replayable. We can conclude that the returned model successfully expresses the core behavior of the process.

To summarize, the results clearly show that high-quality models balancing the different quality aspects can be discovered. There is a significant variance in some of the metrics, particularly precision, indicating that the settings of the algorithm have a notable impact. Our preliminary investigation shows that, based on the event log, certain parameter choices are likely to result in high-quality models. Choosing combined fitness significantly increases the likelihood of the discovered model to contain all or most of the log activities. Our experimentation and analysis give a first indication about which parameters have a more notable impact and whether certain settings are more suitable for logs with certain properties. However, we investigated only four event logs and clearly further experimentation needs to be performed to explore to which degree a generalization of our results is possible. Note that the impact of the candidate traversal order has not been investigated yet, and may allow for further improvements.

8.3. Running Time Analysis

In general, the worst-case running time of the eST-Miner is exponential in the number of log activities A , since $\mathcal{O}((2^{|A|})^2)$ candidate places may have to be evaluated (compare [20]). However, limiting the tree depth to a *fixed* value $2 \leq k \leq |A|$, as was done in the experiments performed in the context of this work, can improve the worst-case running time. In the complete candidate tree the depth of a place coincides with the number of activities connected to that place, i.e., for a place $(I|O)$ at depth k we have that $|I| + |O| = k$. The number of candidate places at depth k corresponds to the number of all possible subsets of A of size k times all possibilities to split them over the sets of ingoing and outgoing transitions (for simplicity, we omit the insignificant border case of empty sets). For a fixed traversal depth of k , in the worst-case we visit all candidates on all levels from 2 to k . Thus, for a fixed traversal depth k the number of place candidates visited in the complete candidate tree is bounded by

$$\sum_{i=2}^k \left(\binom{|A|}{i} \cdot 2^i \right) \leq k \cdot \left(\binom{|A|}{k} \cdot 2^k \right)$$

$$\in \mathcal{O}(k) \cdot \mathcal{O}(|A|^k) \cdot \mathcal{O}(2^k) \subseteq \mathcal{O}(|A|^k) \quad (\text{for fixed } k)$$

We conclude that for a fixed traversal depth of k the number of place candidates evaluated in the worst-case becomes polynomial in the number of activities.

In our experimentation, we chose a fixed tree traversal depth of 5 to make a large-scale experimentation more feasible. We tracked the running times of the various components of the proposed eST-Miner variant with the goal to verify that our newly introduced place selection subroutine does not significantly decrease the algorithm’s performance. In Figure 25, a summary of the running times of the different subroutines is shown on the left. Clearly, the fitness evaluation, i.e., the replay of the event log on each evaluated place candidate, makes up the bulk of the algorithms running time. The time needed for removing implicit places varies a lot over the runs (low values of τ tend to result in more places being inserted and thus more time needed for implicit place removal) but remains insignificant in most cases. Most importantly, in the context of this work, the time spend on place selection is even less than the time spend on computing the place candidates (tree traversal), as can be seen on the right-hand side of Figure 25 (note that the scale is different).

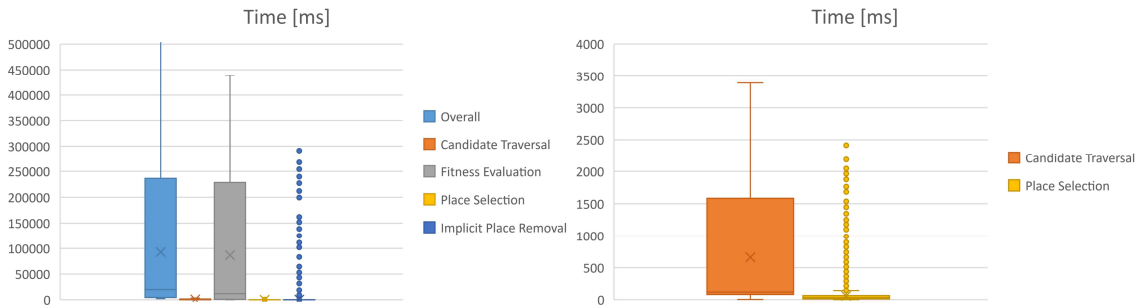


Figure 25. Overview of the running times achieved in our experiments on the left, with a smaller scale visualization of the shorter running times on the right. The newly added place selection subroutine does not add significantly to the overall running time of the algorithm.

9. Discussion and Future Work

The algorithm presented in this work is an extension of the eST-Miner. The goal is to provide fitness guarantees on the returned Petri net while preserving the advantages of the algorithm, such as its ability to reliably discover complex control-flow structures (e.g. long-term dependencies) and to abstract from infrequent behavioral patterns without categorically removing infrequent activities or trace variants. The algorithmic framework we proposed allows for a lot of flexibility in a variety of components

and only a subset of the possible options has been explored in this work. We can imagine several extensions and refinements of the strategies proposed so far.

In Section 5, we introduced a new fitness metric usable within the eST-Mining framework with the goal of avoiding the discovery of places that deadlock infrequent activities. Aggregated fitness does not allow for any place to restrict an activity more than what is allowed according to the noise threshold, which guarantees that no activity can be deadlocked (if $\tau > 0$). Thus, activities get removed from the Petri net only if all the traces that contain them happen to be no longer replayable.

This strategy has the intended positive effect, i.e., our evaluation clearly shows that we succeed in the sense that the models discovered using combined fitness are much more likely to contain all activities from the event log. However, the decision tree analysis shows that we do not necessarily find the best-scoring models using combined fitness, in particular with respect to precision. While inclusion of infrequent but well-defined behavior has been the goal, achieving it results not only in the representation of infrequent but interesting behavioral patterns by the returned process models, but also activities without a well-defined control-flow remain part of the discovered model. The eST-Miner framework connects these activities using the most constraining places allowed, which in the worst-case result in an activity that is enabled by \blacktriangleright , may loop, and gets disabled by \blacksquare . An example for such structures can be seen in Figure 21 for the activities *LacticAcid*, *Leucocytes* and *CRP*. Obviously, such structures have a strong negative impact on precision, even though they seem reasonable in the context of the goals and constraints. Less constraining fitness metrics allow for more restrictive places to be added, which may remove such activities or connect them in a more restrictive way, resulting in higher precision values. Based on the assumption of our user being interested in all activities given in the event log, an investigation of a suitable adaption of aggregated fitness or a post-processing step for more restrictive re-connection of such activities are promising future work.

Fitness metrics diverging significantly from what has been proposed so far may be useful depending on the quality aspects a potential user is interested in. However, to utilize the performance optimization enabled by the eST-Miners complete candidate tree, they must satisfy the monotonicity properties discussed in Section 5. Straightforward relaxations of aggregated fitness such as the average, mean or harmonic mean of the individual fitness of a place's transitions do not satisfy this requirement.

Another interesting topic to investigate is the removal of activities that are no longer part of the replayable event log. In particular, when using combined fitness, this straightforward approach to guarantee deadlock-freeness of the returned may be unnecessarily strict: the removed activity may not be the reason for the trace being unfitting and may not be included in a deadlock at all. Future work includes the investigation of alternative approaches for deadlock detection and prevention that may keep such activities as part of the model.

When using relative or absolute fitness, the fitness definition on the local level is naturally extended to the fitness definition on the global level, i.e., a fraction of replayable traces. When using aggregated fitness this is no longer the case. This makes the use of the algorithm less intuitive for the user, complicates implicit place removal, and, due to the more constraining nature of aggregated fitness, imposes somewhat harder requirements for places to satisfy than when using absolute or relative fitness with the same value of τ . A strategy to consolidate the two views on fitness or the investigation of the impact of using two different fitness thresholds seems worthwhile.

We proposed and evaluated several delta adaption strategies. Unfortunately, no reliable conclusions can be drawn from the experiments performed so far. In particular, the choice between sigmoid and linear adaption functions does not seem to be very impactful for most of the event logs and parameter combinations investigated in this work. However, improvements or variations of these strategies are likely possible. In fact, there is a multitude of options for delta adaption functions which do not necessarily need to be based on the parameters of place complexity, but may incorporate any information available at the place level. Examples include all kinds of relations between or constraints on the connected activities, token behavior and/or attributes of related activities or replayable traces. It would be particularly interesting to investigate to which degree the approach can be used to prioritize non-standard quality aspects, for example related to user interests such as compliance or performance.

There is room for improvement concerning the time performance of the algorithm as well. When an activity is determined to be no longer part of the replayable event log and is therefore removed, all subtrees in the complete candidate tree including this activity may be cut off without impacting the returned model. Furthermore, in this work, we apply the standard ILP-based approach to implicit place removal, which identifies implicit places based on the structure of the Petri net. Unfortunately, this approach becomes very time-consuming for larger sets of places. The replay-based approach introduced in [26] is much faster and can identify most implicit places. However, in the standard eST-Mining framework it does not verify whether all places required to make a currently evaluated place implicit are indeed present in the net, which is incompatible with the use of combined fitness in the framework proposed in this work. An adaption of this implicit place removal strategy may contribute to the overall performance of the proposed eST-Miner variant.

10. Conclusion

In this paper, we proposed various extensions to the eST-Miner. We introduced a new fitness metric, aggregated fitness, investigated its properties and showed that it can be incorporated into the eST-Mining framework. The goal of this metric is to improve the eST-Miner's place evaluation to avoid the discovery of places that prevent infrequent activities from being executed categorically, while maintaining its ability to abstract from infrequent behavioral patterns.

Furthermore, we propose a framework for place selection with the goal of guaranteeing that the discovered Petri net is free of deadlocks and satisfies a user-definable minimal fitness constraint. The approach employs heuristics to efficiently select a suitable subset of the discovered fitting places, while aiming towards high precision and simplicity. The algorithm is capable of discovering complex control-flow structures such as non-local dependencies. Furthermore, it is able to abstract from infrequent behavioral patterns in the event log without simply filtering out infrequent activities or trace variants and to provide guarantees without over- or underfitting.

Our experiments, using four different event logs, clearly show that not only is it possible to discover high-quality models using the introduced approach, but also the heuristics applied have a significant impact on the obtained Petri net. Based on the parameter settings, models with a very different focus with respect to fitness, precision and the handling of infrequent behavior can be discovered. Some parameters have a stronger effect than others and some parameter choices seem to be more suitable for logs with certain properties, which should be verified by further experimentation.

A theoretical analysis of the running time, as well as an experimental overview of the time needed for the various subroutines of the algorithm, was presented, followed by a discussion of design decisions, open questions and future work.

Besides the aspects discussed in detail in Section 9, future work includes further experimentation to explore the generalization of the presented preliminary results, as well as the impact of the candidate place traversal order and its interaction with the heuristics used. The dead transitions removed from the model because they are no longer part of the replayable event log give rise to further possible extensions of the eST-Miner. When detected early on, they can be used to identify and cut off candidate subtrees consisting of dead places to improve the running time. Further investigation into the cause of their removal may lead to better noise handling strategies to improve the quality of discovered models. Finally, it would be interesting to investigate whether the presented place selection strategies can be adapted to improve other algorithms as well.

Acknowledgments: Special thanks go to Tobias Brockhoff for his support with conducting the presented experiments. We thank the Ministry of Culture and Science of the German State of North Rhine-Westphalia (MKW) and the Excellence Strategy of the Federal Government and the Länder for supporting our research.

References

- [1] Reisig W. *Understanding Petri Nets: Modeling Techniques, Analysis Methods, Case Studies*. Springer Berlin Heidelberg, 2013. ISBN 9783642332784.
- [2] Desel J, Oberweis A, Reisig W, Rozenberg G. *Petri nets and business process management*. Saarbrücken: *Geschäftsstelle Schloss Dagstuhl*, 1998.
- [3] Desel J, Esparza J. *Free-Choice Petri Nets*. Cambridge Tracts in Theoretical Computer Science. Cambridge University Press, 1995. ISBN 9780521465199.
- [4] Berthelot G. Transformations and Decompositions of Nets. In: *Petri Nets: Central Models and Their Properties*. Springer, Berlin, Heidelberg, 1987 pp. 359–376.
- [5] Wen L, van der Aalst WMP, Wang J, Sun J. Mining process models with non-free-choice constructs. *Data Mining and Knowledge Discovery*, 2007. **15**(2):145–180.
- [6] Leemans S, Fahland D, van der Aalst W. Discovering Block-Structured Process Models from Event Logs - A Constructive Approach. *Application and Theory of Petri Nets and Concurrency*, 2013.
- [7] Weijters AJMM, Ribeiro JTS. Flexible Heuristics Miner (FHM). In: *Proceedings of the IEEE Symposium on Computational Intelligence and Data Mining, CIDM 2011*, part of the IEEE Symposium Series on Computational Intelligence 2011, April 11-15, 2011, Paris, France. IEEE, 2011 pp. 310–317.
- [8] Badouel E, Bernardinello L, Darondeau P. *Petri Net Synthesis*. Text in Theoretical Computer Science, EATCS Series. Springer, 2015.
- [9] Lorenz R, Mauser S, Juhás G. How to Synthesize Nets from Languages: A Survey. In: *Proceedings of the 39th Conference on Winter Simulation: 40 Years! The Best is Yet to Come, WSC '07*. IEEE Press, Piscataway, NJ, USA, 2007 pp. 637–647.

- [10] Bergenthum R, Desel J, Lorenz R, Mauser S. Process mining based on regions of languages. *Proc. 5th Int. Conf. on Business Process Management*, 2007. pp. 375–383.
- [11] van der Werf JM, van Dongen B, Hurkens C, Serebrenik A. Process Discovery Using Integer Linear Programming. In: *Applications and Theory of Petri Nets*. Springer, Berlin, Heidelberg, 2008 .
- [12] van Zelst S, van Dongen B, van der Aalst W. Avoiding Over-Fitting in ILP-Based Process Discovery. In: *Business Process Management*. Springer International Publishing, Cham, 2015 pp. 163–171.
- [13] van Zelst S, van Dongen B, van der Aalst W. ILP-Based Process Discovery Using Hybrid Regions. In: *ATAED@Petri Nets/ACSD*. 2015 .
- [14] Carmona J, Cortadella J, Kishinevsky M. A region-based algorithm for discovering Petri nets from event logs. In: *Business Process Management*. Springer, 2008 p. 358–373.
- [15] Darondeau P. Deriving unbounded Petri nets from formal languages. In: *CONCUR'98 Concurrency Theory*. Springer, Berlin, Heidelberg. ISBN 978-3-540-68455-8, 1998 pp. 533–548.
- [16] Bergenthum R, Desel J, Lorenz R, Mauser S. Synthesis of Petri Nets from Finite Partial Languages. *Fundam. Informaticae*, 2008. **88**(4):437–468.
- [17] Ehrenfeucht A, Rozenberg G. Partial (set) 2-structures. *Acta Informatica*, 1990. **27**(4):343–368.
- [18] Carmona J, Cortadella J, Kishinevsky M, Kondratyev A, Lavagno L, Yakovlev A. A Symbolic Algorithm for the Synthesis of Bounded Petri Nets. In: van Hee KM, Valk R (eds.), *Applications and Theory of Petri Nets*. Springer Berlin Heidelberg, Berlin, Heidelberg. ISBN 978-3-540-68746-7, 2008 pp. 92–111.
- [19] Kalenkova A, Carmona J, Polyvyanyy A, La Rosa M. Automated Repair of Process Models Using Non-Local Constraints. In: *Application and Theory of Petri Nets and Concurrency*. Springer-Verlag, Berlin, Heidelberg. ISBN 978-3-030-51830-1, 2020 p. 280–300.
- [20] Mannel LL, van der Aalst WMP. Finding Complex Process-Structures by Exploiting the Token-Game. In: Donatelli S, Haar S (eds.), *Application and Theory of Petri Nets and Concurrency - 40th International Conference, PETRI NETS 2019, Aachen, Germany, June 23-28, 2019, Proceedings*, volume 11522 of *Lecture Notes in Computer Science*. Springer, 2019 pp. 258–278.
- [21] Mannel LL, van der Aalst WMP. Discovering Process Models with Long-Term Dependencies While Providing Guarantees and Handling Infrequent Behavior. In: Bernardinello L, Petrucci L (eds.), *Application and Theory of Petri Nets and Concurrency - 43rd International Conference, PETRI NETS 2022, Bergen, Norway, June 19-24, 2022, Proceedings*, volume 13288 of *Lecture Notes in Computer Science*. Springer, 2022 pp. 303–324.
- [22] van der Aalst WMP. Discovering the "Glue" Connecting Activities - Exploiting Monotonicity to Learn Places Faster. In: *It's All About Coordination - Essays to Celebrate the Lifelong Scientific Achievements of Farhad Arbab*. 2018 pp. 1–20.
- [23] Garcia-Valles F, Colom J. Implicit places in net systems. *Proceedings 8th International Workshop on Petri Nets and Performance Models*, 1999. pp. 104–113.
- [24] Berthomieu B, Botlan DL, Dal-Zilio S. Petri Net Reductions for Counting Markings. In: Gallardo M, Merino P (eds.), *Model Checking Software - 25th International Symposium, SPIN 2018, Malaga, Spain, June 20-22, 2018, Proceedings*, volume 10869 of *LNCS*. Springer, 2018 pp. 65–84.
- [25] Colom J, Silva M. Improving the linearly based characterization of P/T nets. In: *Advances in Petri Nets 1990*. Springer, Berlin, Heidelberg, 1991 pp. 113–145.

- [26] Mannel LL, Bergenthum R, van der Aalst WMP. Removing Implicit Places Using Regions for Process Discovery. In: Proceedings of the International Workshop on Algorithms & Theories for the Analysis of Event Data (ATAED) 2020, volume 2625. CEUR-WS.org pp. 20–32.
- [27] van Dongen B, de Medeiros A, Verbeek H, Weijters A, van der Aalst W. The ProM Framework: A New Era in Process Mining Tool Support. In: Applications and Theory of Petri Nets 2005. Springer, Berlin, Heidelberg, 2005 pp. 444–454.
- [28] van der Aalst W. Process Mining: Data Science in Action. Springer, Heidelberg, 2 edition, 2016.
- [29] Carmona J, van Dongen B, Solti A, Weidlich M. Conformance Checking - Relating Processes and Models. Springer, Cham, 2018.
- [30] Mannhardt, F. Sepsis Cases - Event Log, 2016.
- [31] De Leoni, M, Mannhardt, F. Road Traffic Fine Management Process, 2015.
- [32] van der Aalst WMP. Spreadsheets for BPM. *Business Process Management Journal*, 2010. **24**:105–127.
- [33] Adriansyah A. Aligning observed and modeled behavior. Ph.D. thesis, Mathematics and Computer Science, 2014.
- [34] Munoz-Gama J, Carmona J. A Fresh Look at Precision in Process Conformance. In: BPM, volume 6336. ISBN 978-3-642-15617-5, 2010 pp. 211–226.
- [35] Tax N, Sidorova N, van der Aalst WMP. Discovering more precise process models from event logs by filtering out chaotic activities. *J. Intell. Inf. Syst.*, 2019. **52**(1):107–139.